UNIVERSITY OF CALIFORNIA,
MERCED

Population genetic analysis of the intertidal limpet *Lottia scabra* and inference of the causes and mechanisms of range limits.

THESIS

submitted for the requirements
for the degree of

MASTER OF SCIENCE
in
Individual Graduate Program
with an emphasis in Quantitative and Systems Biology

by

Joan M. Lehman

Thesis Committee:
Assistant Professor Michael N Dawson, UCMerced, Chair
Assistant Professor Andres Aguilar, UCMerced
Assistant Professor Lara M. Kueppers, UCMerced
Professor Stephen C. Hart, UCMerced

2010

Dedication

To

My beloved family and dear friends.

Special thanks to my husband, Craig Lehman, for his patience in putting up with all the working weekends, and for supporting me during the tough times.

To my parents, family, especially my sisters and my aunt, Jean Laird, thanks for all your help and support. Special gratitude and appreciation to my children and their significant others, Derek and Kerry Lehman, Elizabeth and Keith Hanley, Jennifer Lehman and Brett Walker, for emotional support, listening time, understanding, and sticking with me through thick and thin. Thanks to my friends, who are too many to name here, but especially Diane Lucas, Mary Ormonde, Rusty and Alicia Baez, and Pat Smith, who remind me of who I am, give me a solid foundation and set me straight. Thanks to all for your confidence, encouragement, and advice, and telling me that I can do it when I'm sure I can't.

I would like to express the deepest appreciation to my advisor, Dr. Michael N Dawson, Merced, for all your knowledge, support, advice, and the generosity of your time.

Thanks to all my labmates, Liza Gómez-Daglio, Holly Swift, Lauren Schielbelhut, Miguel Fernandez, Julia Vo, Dr. Keith Bayha, Sharon Patris, Sarah Abboud, Anna Nandipati, and especially Dr. Cynthia Hays, Merced. Thanks for lab support and help with data analysis methods, feedback, emotional support, and sometimes hugs.

Special thanks to Dr. Micha Miller, Columbia College, Sonora CA, for talking me out of quitting when I hit the wall.

TABLE OF CONTENTS

		Page
LIST OF FIGURES		vi
LIST OF TABLES		vii
ABSTRACT OF THESIS		viii
INTRODUCTION		1
CHAPTER 1:	Methods and Materials	5
	Specimen collection	5
	DNA purification, PCR, and sequencing	6
	Sequence analyses	9
	Environmental Pattern	12
CHAPTER 2:	Results	14
	Phylogeography to understand evolutionary history	15
	Genetic diversity	17
	Environmental pattern	29
CHAPTER 3:	Discussion	42
	Evolutionary history from phylogeography	42
	Inferring process from environmental pattern	43
	Causes of range limits from predicted characteristics	46
CHAPTER 4:	Conclusion	50
ACKNOWLEDGMENTS		53
REFERENCES		54
APPENDIX		58

LIST OF FIGURES

		Page
Figure 2.1	Map of locations	21
Figure 2.2	Haplotype networks	22
Figure 2.3	Abundance	23
Figure 2.4	Slatkin's linearized F_{ST}	24
Figure 2.5	Proportion of alleles	25
Figure 2.6	Number of alleles	26
Figure 2.7	Haplotype diversity	27
Figure 2.8	Nucleotide diversity	28
Figure 2.9	Air temperature	35
Figure 2.10	Precipitation	36
Figure 2.11	Vapor pressure deficit	37
Figure 2.12	Total daily incident shortwave flux	38
Figure 2.13	Salinity	39
Figure 2.14	Sea surface temperature	40
Figure 2.15	Concentration of chlorophyll-*a* in sea water	41

LIST OF TABLES

		Page
Table 1.1	Hypothesized causes of range limits	3
Table 4.1	Conclusion for range limits	51
Table S1	Site locations, GPS coordinates, and sample size	58
Table S2	Genetic diversity table	59
Table S3	Environmental conditions for range areas	60

ABSTRACT OF THE THESIS

Population genetic analysis of the intertidal limpet *Lottia scabra* and inference of the causes and mechanisms of range limits.

By

Joan M. Lehman

Master of Science
in
Individual Graduate Program
with an emphasis in Quantitative and Systems Biology

University of California at Merced, 2010

Assistant Professor Michael N Dawson, UCMerced, chair

Range limits have been described for many species, and the interest in range limits has increased in the wake of climate change, but few researchers attempt to document the causes and mechanisms of these limits and empirical tests of range limit theory remain sparse. Three principle mechanisms have been proposed to limit species' range in models incorporating environmental heterogeneity and evolution: genetic impoverishment, migration load, or a physical barrier to dispersal. Other possibilities include a "leaky" barrier and secular migration. Here, I describe the distribution, abundance, genetic variation in partial 16S and cytochrome *c* oxidase subunit I mitochondrial loci, and environment of the low to medium dispersal species *Lottia scabra*, an intertidal limpet with a range from Oregon, USA, to Baja California, Mexico, that crosses a known biogeographic break at the region on Point Conception, CA. The environmental variables describe latitudinal geographic variation of air temperature, precipitation, vapor pressure deficit, solar radiation, salinity, sea surface temperature, and concentration of chlorophyll-*a* in sea water. I found *L. scabra* is comprised of two, not one, evolutionary lineages: the North Clade from 43.3^{o}N to 34.5^{o}N, and the South Clade from 35.7^{o}N

to 29.9°N. I found high gene flow and low to medium genetic diversity within both the North and South Clades, high upwelling and cold temperatures at the northern limit of the North Clade, and a pronounced decrease in chlorophyll-*a* with an increase in sea surface temperature at the southern limit of the North Clade. I found the likely cause of the northern range limit of the North Clade was migration load with recruitment limitation, and two plausible causes for the southern range limit of the North Clade and the northern range limit of the South Clade: migration load and/or a "leaky" barrier.

Keywords: limpet, dispersal, geographic range limits, intertidal species, migration load, "leaky" barrier

INTRODUCTION:

The coincidence of climate change and shifting species boundaries has spurred a resurgence in the study of intertidal species range limits (Jones et al., 2009; Kuo and Sanford, 2009; Pitt et al., 2010). The range, or geographical distribution, is the totality of the physical space where a population affected by biotic and/or abiotic factors, which constitute its niche, persists. At the range edge, or limit, where the local population dynamics change to the extent that the population is unable to exist beyond this point (Gaston, 2003), populations are simultaneously affected by evolutionary (e.g., Hoffmann and Blows 1993; Kirkpatrick and Barton, 1997) and ecological processes (e.g., Parmesan and Yohe, 2003; Helmuth et al., 2005).

Range dynamics incorporate environmental instability, dispersal rates, and niche requirements of the species range (Holt, 2003). A spatially complex balance of local adaptation and gene flow exists at the periphery where small changes in environment can dramatically shift this balance (Kirkpatrick and Barton, 1997). Range limits therefore will remain stable until a 'tipping point' is reached where the joint impact of all worsening vital rates of survival, growth, and reproduction overwhelms the collective effect of all rates that improve, depending on the importance of the influence of each condition on the overall population growth (Doak and Morris, 2010). For example, genetic variance can have little effect on the range size if strong gene flow from the center of the range inhibits adaptation at the periphery, and in the absence of environmental change, this maladaptation prevents the range from expanding outward with the periphery acting as a demographic sink (Mayr, 1963; Hoffmann and Blows, 1994; Kirkpatrick and Barton, 1997).

Understanding the causes of range limits is crucial because among intertidal invertebrates along the Northeast Pacific coast changes in abundance may be related to changes in geographic

ranges where at Hopkins Marine Lab, most southern species have increased in abundance and most northern species have decreased (Sagarin et al., 1999), suggesting climate change is the underlying driver (Parmesan and Yohe, 2003). Latitudinal gradients such as temperature in the ocean (Banks et al., 2010; Dawson et al., 2010) can strongly influence the geographic distribution of marine invertebrates, particularly as a species approaches its range limit, but little is know about the mechanisms involved in range limits.

Three principal mechanisms have been proposed to limit species' ranges in models incorporating environmental heterogeneity and evolution: genetic impoverishment, migration load, or a physical barrier to dispersal (Holt, 2003; Sexton et al., 2009; Table 1.1A). A fourth hypothesis of a "leaky" barrier (Schoch et al., 2006). Genetic impoverishment occurs when populations at the border must be sustained largely by self-recruitment, and adaptation is limited by the availability of heritable genetic variance. Migration load occurs when high influx of locally maladaptive alleles may constrain the response to selection. With a physical barrier to dispersal, organisms are prevented from entering locations beyond the boundary, which isolates populations and/or communities, while a "leaky" barrier results in distinctly different communities because of the presence of taxa with life histories sensitive to the magnitude of the barrier (Schoch et al., 2006). An alternate possibility (Table 1.1B,) is 'secular migration' (Lomolino et al. 2005: p. 154), where the predicted characteristics of the hypothesis occur when moderate gene flow introduces intermediate levels of genetic variance thus increasing evolutionary potential (Ellstrand and Elam 1993; Gomulkiewicz et al., 1999) and enabling gradual evolution of the species range with no long-term range limit (Mayr, 1963). Although secular migration suggests no long-term range limit, such species will appear to have a range limit when observed for a snapshot in evolutionary time.

Table 1.1: Predicted characteristics of populations at the border of a species' range under four hypothesized causes of range limits. (Modified from Dawson et al., 2010).

A	**H_1: Genetically impoverished isolated population**	**H_2: Migration load**	**H_3: Physical barrier to dispersal**	**H_4: Leaky barrier to dispersal with frequent immigration**	B	**H_{SM}: Secular migration (moderate gene flow)**
Characteristics of environment (biotic or abiotic)					***Characteristics of environment***	
i. Environmental change at margin	Gradual change	Gradual change	Dispersal route blocked/broken	Dispersal route mostly blocked	i. Environmental change at margin	Gradual, stepped, or abrupt change
Size of marginal population					***Size of marginal population***	
ii. Marginal population size	Small	Declining toward border	Large	Large changing to small	ii. Marginal population size	Moderate – large
Border populations					***Border populations***	
iii. Gene flow	Low	High	Low/medium/high	Low	iii. Gene flow	Medium
iv. Genetic diversity	Low, decreasing toward margin	High	Medium/high	Low	iv. Genetic diversity	Moderate
v. Unique alleles	Prevalent	Few	Few/some	Few/some	v. Unique alleles	Some

Although many theoretical models exploring possible causes of range limits have been developed during the past several decades, empirical tests of range limit theory remain sparse (Sexton et al., 2009). Recent empirical population genetic studies have shown very high dispersal in two rocky intertidal marine invertebrates, the volcano barnacle *Tetraclita rubescens* (Dawson et al., 2010) and the sea urchin *Centrostephanus rodgersii* (Banks et al., 2010), whose poleward geographic ranges are limited by sea surface temperature (SST). The inferred causes of these range limits include migration load (Banks et al., 2010; Dawson et al., 2010), a lack of relevant heritable genetic variance, and/or genetic trade-offs (Banks et al., 2010). Because each of these three genetic mechanisms would cause range expansion or contraction with changing environmental conditions, but not evolution of the range limit, they are implicated as the causes

of the largely synchronous multi-species range expansions that have been observed in recent decades (Parmesan and Yohe, 2003; Perry et al., 2005).

In *T. rubescens* the data suggests that migration load, when alleles that might adapt to new environments are swamped by maladapted genes from high gene flow, is the primary factor setting the northern range limit, but does not prove the absence of heritable genetic variation (Dawson et al., 2010). While migration load is associated with high gene flow and high genetic diversity, lower genetic diversity with less gene flow is expected for low to medium dispersal species. In low dispersal species, which have local adaptation, selection is expected to be a stronger force than dispersal ability and it is expected that different patterns will emerge at the range boundaries.

In the low-medium dispersal species *Lottia scabra*, individual performance of adults was not reduced in marginal populations in the northern population (Gilman, 2006a), suggesting the range boundary is controlled by a process that operates on recruitment rather than performance, and the underlying mechanism may be biological, such as reproductive failure (Hutchins, 1947), or physical, such as oceanographic dispersal limitation (Gaylord and Gaines, 2000). *L. scabra* is a common herbivorous patellogastropod (limpet) middle-high rocky intertidal species found along the Northeastern Pacific coast of North America from southern Oregon (43^{o} 20'N) to approximately central Baja California, Mexico (28^{o}N); (Morris et al., 1980). This species has a lecithotrophic (larvae live off yolk supplied with the egg) pelagic larval duration of less than 14 days (Strathmann, 1987), a benthic adult phase of 10 to 30 years, and the major period of settling occurs from July to October in organisms at 38^{o}N (Sutherland, 1970).

Here, I test the hypothesized causes of range limits of *L. scabra* with genetic analysis and comparison of patterns of environmental conditions. The first hypothesis, genetically

impoverished isolated population (Table 1.1, H_1), predicts gradual environmental change at margin, a small marginal population size, low gene flow and prevalent unique alleles at the border, with low or decreasing genetic diversity toward the margin (Dawson et al., 2010). The second hypothesis, migration load (Table 1.1, H_2), predicts gradual environmental change at margin, a marginal population that declines towards the border, with high gene flow, high genetic diversity, and few unique alleles in the border populations (Dawson et al., 2010). The third hypothesis, physical barrier to dispersal (Table 1.1 H_3), predicts a broken or blocked route to dispersal at the range limit, a large marginal population, with low to high gene flow, medium or high genetic diversity, and few or some unique alleles (Dawson et al., 2010). A "leaky" barrier (Table 1.1 H_4) has the dispersal route mostly broken, a large population size changing rapidly to small at the edge, low gene flow and genetic diversity, and few/some unique alleles (Sarah E. Gilman, Claremont Colleges, California, USA; personal communication, 2010). Secular migration (Table 1.1, H_{SM}), predicts gradual, stepped, or abrupt environmental change at the margin with a moderate to large marginal population size, border populations that have medium gene flow, moderate genetic diversity, and some unique alleles (Dawson et al., 2010).

MATERIALS AND METHODS:

Specimen collection

Fifteen specimens of *L. scabra* were collected (except where rare) between 1996-2009 at 70 locations in Oregon, USA, California, USA and Baja California, Mexico spanning the majority of the species' range (Fig. 2.1, Table S1). Specimens were selected haphazardly, and collected by hand, to represent the range of individual sizes and tide height location found at each site.

Tissue archives are curated in Michael N Dawson's laboratory at the University of California at Merced and stored at -4ºC.

DNA purification, PCR, and sequencing

DNA was extracted from a few-millimeter^3 piece of foot muscle and/or mantle tissues using a CTAB-Phenol/Chloroform (PCI) based protocol (Dawson et al., 1998), or the Qiagen DNeasy tissue kit (http://www.qiagen.com). The PCI extractions were eluted in 50-100 µl 10 mM Tris-HCL pH 8.3. Qiagen extractions followed the manufacturer's instructions except for the spin-down after adding 500 µl Buffer AW2, which was centrifuged for 2 minutes (min) at 14,000 g, then the flow-through was discarded followed by an additional centrifuge of 1 min at 14,000 g. For elution, 100 µl Buffer AE was used and incubated for 2 min at room temperature before final spin-down. Quantification of extractions was checked on gels using 1 µl 6X dye and 3 µl sample against a DNA standard ladder (GeneRuler ™100 bp DNA Plus Ladder; Fermentas; Ontario, Canada) on a 1.4% agarose in 0.5x TBE minigel run at 160V for 25 min. The gel was stained with a mixture of 1 µl Gelstar (http://www.gelstar.com) to 1 ml H_20 for 25 min and photographed.

For polymerase chain reactions (PCR), the mitochondrial markers partial cytochrome *c* oxidase subunit I (COI) and partial mt16S were amplified and sequenced. Amplification was done using an Applied Biosystems (ABI) 2720 thermal cycler or ABI 9600 thermal cycler, (www.appliedbiosystems.com; Applied Biosystems, Foster City, California, USA), under various conditions (listed below). All samples were sequenced in both forward and reverse directions for COI. For 16S, after multiple samples were sequenced, forward sequencing was determined to be sufficient. PCR was performed in 50 µl total volumes with the following

components: 1 µl DNA template (from purified DNA solutions), 35.40 µl dH_20, 5 µl 10X buffer and 5 µl (3 mM) $MgCl_2$, (Applied Biosystems, Foster City, California, USA), 1 µl 10 mM (0.2 mM) dNTPs, 1.25 µl of each primer at 20 µM. (3 mM $MgCl_2$ primers at final concentration 0.5 µM), and 0.1 µl (0.5U) Taq (AmpliTaq® DNA Polymerase, Applied Biosystems, Foster City, CA). The primers were locus-specific as described below (Operon, Huntsville, Alabama, USA).

Primers for amplifying COI were designed from preliminary sequences amplified using HCO2198 with LCO1490 (Folmer et al., 1994) or an exploratory primer Ls_LCO1588 (5'-TAATACACACRGGWACAGG) designed using the *Lottia digitalis* whole mitochondrial genome (Simison et al. 2006) and other published sequences for *Lottia fenestrata* (PSN_0601; Eernisse et al. unpublished data), *Acmaea mitra* (GenBank_accession: AF242036), *Lottia paradigitalis* (AF295538), *Lottia strigatella* (AF295539), *Notoacmea fascicularis* (AF130120), *Patella aspera* (PAS291547), *Patelloida saccharina* (AY628320), and *Tectura testudinalis* (AF242065). The *L. scabra* specific primers used for COI were Ls_LCO1588e (5'-TAATACACACRGGWACAGGRYTCCTAA) and Ls_HCO2166 (5'-GGTGTTGGAATAGGACAGGGTCTCC). The PCR consisted of six steps of 94°C for 8 min, 58°C for 1 min, 72°C for 2 min, 94°C for 4 min, 57°C for 1 min, 72°C for 1.5 min, then 35 cycles of 94°C for 45 seconds (s), 56°C for 45 s, and 72°C for 75 s, followed by an extension step at 72°C for 10 min; the reaction was terminated by cooling to 4°C, or with a touchdown of 94°C for 8 min, 52°C for 1 min, 72°C for 2 min, 94°C for 4 min, 51°C of 1 min, and 72°C of 2 min, followed by 35 cycles of 94°C for 45 s, 50°C for 45 s, and 72°C for 75 s with a final hold of 72 °C for 10 min then 4°C until end. For difficult samples, LCO1490 and HCO2198 (Folmer et al., 1994) primers were tried with a touchup of 94°C for 8 min., 48°C for 2 min., 72°C for 2 min, 94°C for 4 min, 49°C for 2 min, and 72°C for 2 min, followed by 35 cycles of 94°C for 45 s,

50°C for 45 s, and 72°C for 75 s with a final hold of 72 °C for 10 min then 4°C until end, or other primers designed for difficult samples were tried, LsCOI_1610f (5'-CCGTTGTAACAGCACAC GC) and LsCOI_2166r_short (5'-GGAATAGGACAGGGTCTCC) with a touchup of 94°C for 8 min, 50°C for 2 min, 72°C for 2 min, 94°C for 4 min, 51°C for 2 min, and 72°C for 2 min, followed by 35 cycles of 94°C for 45 s, 52°C for 45 s, and 72°C for 1 min with a final hold of 72 °C for 10 min, then 4°C until end.

For 16S, the universal primers 16Sar and 16Sbr (Palumbi, 1996) were used to generate preliminary sequence data, which were then used to design the specific primers Ls16Sf (5'-CCTCCGCACATCCCTTACG) and Ls16Sr (5'-GGCTTTAATGGTCGAACAGACC) for use in PCR. The PCR consisted of six steps of 94^{o}C for 8 min, 55^{o}C for 2 min, 72^{o}C for 1.5 min, 94^{o}C for 4 min, 56^{o}C for 1.5 or 2 min, 72^{o}C for 75s, then 35 cycles of 94^{o}C for 45s, 57^{o}C for 45s, and 72^{o}C for 60s, followed by an extension step at 72^{o}C for 10 min; the reaction was terminated by cooling to 4^{o}C. For difficult samples, Hydro16Sar (5'-TCGACTGTTTACCAAAAACATAG C) and Hydro16Sbr (5'ACGGAATGAACTCAAATCATGTAAG); (Cunningham and Buss, 1993) primers were tried with a touchup of 94°C for 8 min, 52°C for 2 min, 72°C for 90s, 94°C for 4 min, 53°C of 90s, and 72°C of 75s, followed by 35 cycles of 94°C for 45s, 54°C for 45s, and 72°C for 60s with a final hold of 72 °C for 10 min then 4°C until end.

PCR products of 45 to 47 µl were purified by the author for sequencing by incubating product with 4 µl Exonuclease I (USB Corporation, Cleveland) and 4 µl Shrimp Alkaline Phosphatase (USB Corporation, Cleveland) at 37°C for 15 min, 80°C for 15 min, then 4°C. until end, or purified by the sequencing facility (see below). The concentration of DNA in the purified PCR was quantified by the same electrophoresis protocol as the DNA extractions.

DNA concentration was adjusted to required specifications for each facility, and sent to one of two outside facilities for sequencing with 3.0 μM PCR primers. UC Davis sequencing facility (http://www.davissequencing.com/) utilizes ABI BigDye Terminator v3.1 Cycle Sequencing chemistry on an ABI 3730 Capillary Electrophoresis Genetic Analyzer (Applied Biosystems, Foster City), and University of Washington High-Throughput Genomics Unit facilities, which utilizes high-throughput capillary sequencer (http://www.htseq.org/aboutUs.html). PCR primers were used for all sequencing reactions.

Sequence analyses

Sequencher v4.9 (Gene Codes Corporation, Ann Arbor, Michigan, USA) was used to assemble all electropherogram trace files into contigs by individual, if forward and reverse sequences were available, and then by population where sequences from all the specimens collected from a single location were then assembled into a single site-contig. All autapomorphies and synapomorphic positions were checked and corrected if necessary in the original specimen-contigs. All sequences were edited by eye to remove all primer sequences, and at both stages, polymorphic sites were inspected by eye and base calls corrected if necessary. The corrected specimen-contigs were then exported in FASTA-concatenated format with options of current orientation, upper case, without converting all ambiguities.

Each individual's sequence for 16S was then converted to MSDOS FASTA format files for import into ClustalX 2.0.12 (Jeanmougin et al., 1998) in which they were aligned using default gap-opening and gap-extension weighting and then exported as a NEXUS file. The COI sequences were exported from Sequencher as text files and the unaligned dataset was assembled in Sequence Alignment Editor Se-Al v2.0a11 (http://tree.bio.ed.ac.uk/software/seal). All

sequences were then assembled and aligned manually using Se-Al v2.0a11 and opened in MacClade 4.08 OS X (Sinauer Associates, Sunderland, MA, USA), to save as non-interleaved text. The files were then opened in Textmate 1.5.9 (http://macromates.com), and for mt16S and mtCOI the ends were trimmed of missing or uninformative nucleotide positions and a total of 520 characters for 16S and 530 characters for COI were used in the analysis.

Highly divergent sequences were examined in BLAST (http://blast.ncbi.nlm.nih.gov/Blast.cgi), and if identification was still in question the individual shells were re-examined. Some specimens were determined to have been misidentified at collection and to be species' other than *L. scabra* are not included in this dataset. Other sequences showed evidence of possible heteroplasmy or hybridization and are to be analyzed at a later date and are not included in this dataset. Other extremely short sequences resulting from PCR and sequencing error were excluded from the dataset.

I tested the presence of statistically dissimilar phylogenetic signals in 16S and COI using the Partition Homogeneity Test in PAUP* 4b10 (Swofford, 2002) applying unweighted maximum parsimony, gaps as 5th bases, starting tree obtained via stepwise addition, TBR, initial 'MaxTrees' setting = 100, heuristic search with 100 replicates. If the test determines that the two markers, 16S and COI, do not reveal the same structure, analysis proceeded as separate markers.

Statistical parsimony mitochondrial haplotype networks were drawn with TCS v1.21 (Clement et al., 2000) coding gaps as a fifth state, 95% connection confidence to estimate haplotype (allele) outgroup probabilities, with sequences with missing positions at the end of the matrix in increasing order of missing data (Joly et al., 2007).

I assessed the data separately using the entire sequence dataset, and the dataset with the missing/ambiguous nucleotide positions excluded in PAUP*, and reran the subset in TCS.

Fourteen 16S sequences with both missing and multiple ambiguities were problematic and brought into question the most parsimonious connections between the major clades when comparing the two haplotype networks, so these sequences were excluded from the final dataset. Only specimens that had both 16S and COI sequences were analyzed. Network graphs were redrawn in Adobe Illustrator CS3 13.0.2 (1999-2002 Microsoft Corporation) using pie charts from Microsoft Excel 2008 (www.microsoft.com).

Due to unequal sample sizes, I ran correlation tests to determine whether sample size influenced measures of genetic diversity. I used these analyses to determine the minimum number of sequences that would represent each population in subsequent analyses by plotting the frequency of diversity with the number of sequences. It was determined that a population of at least 8 individuals did not bias diversity downwards when compared with larger sample sizes, but that all locations with less than 8 samples should be excluded.

To determine isolation by distance, calculations for Slatkin's linearized F_{ST} was generated in Arlequin v.3.5 (Excoffier and Lischer, 2010) for all pairs of populations as $t/M=FST/(1-F_{ST})$ with deletions, tranversions and transitions weighted 1, number of permutations for significance was 100 and number of permutations for Mantel Test was 1000. I assessed genetic variation within the mtDNA loci at nucleotide, haplotype, location, and sample levels using "standard" and "molecular" diversity indices in Arlequin v.3.5. In Arlequin, I inferred haplotypes from genetic distances (pairwise sequence difference), transitions and transversions both weighted 1 when all missing positions were excluded with 'allowed missing level per site' = 0.0. To assess latitudinal variation, number of alleles, haplotype diversity, and nucleotide diversity were plotted against distance from the southern range limit for the North Clade, and the northern range limit for the South Clade, with a running mean of 50 km with sites

that had 5 or more samples within 100 km of each other.

Species abundance data was requested from Coastal Biodiversity Surveys (CBS) (http://cbsurveys.ucsc.edu). Abundance was measured using 50 x 50 centimeter (cm) quadrats divided into three regions across the intertidal area representing high, mid, and low zone tidal biology resulting in a maximum of 33 plots (http://cbsurveys.ucsc.edu/sampling/mobiles.html). Due to the presence of the sister taxon *Lottia conus,* a likely competitor (D. Eernisse, California State University at Fullerton, USA; personal communication, 2010), which is highly similar in appearance to *L. scabra* and whose abundance increases towards the south beginning at approximately site 39-USCARSB until *L. conus* becomes common south of site 54-USCACCO and dominates in the region of site 65-USCAScS, the abundance data of the southern clan east and south of site 39-USCARSB can only be used as a composite of the two species, so is not included in this analysis.

Environmental pattern

Monthly averages were calculated for all environmental measurements at each collection site for all years available, from 1913 to 2010, and minimum, mean, median, and maximum values were calculated for all sites for all months. Site coverage for sea surface temperature (SST), (http://coastwatch.pfeg.noaa.gov/erddap/griddap/erdPHsstamday.html) was 100%, and Daymet (http://www.daymet.org/) environmental data, was 89%. Latitudinal variation plots were made for June and December for all environmental conditions, except for salinity, which had poor coverage. To more closely match coverage for salinity, I averaged May, June, and July for a proxy for June increasing site coverage from 50% to 76%; and November, December, and January for a proxy for December increasing site coverage from 31% to 67%.

Point Distance was generated inside the Spatial Analyst extension of ARCGISv.10 (http://www.esri.com) for all combinations of locations and measured in North America Equidistant Conic Projection in meters for straight distances; then the shortest oceanic distance was calculated for each.

Air temperature, precipitation, vapor pressure deficit, and total daily incident shortwave radiation flux density was calculated from Daymet. Daymet generates daily interpolated surface weather variations over the conterminous USA. Location point coordinates were used to access all daily data taken as an average over the daylight period of the day from 1980 to 2003, for 365 days a year, from the nearest 1 x 1 kilometer (km) Daymet gridcell. Data was averaged for each month per year, and then if no data was available, longitude or latitude was modified slightly towards the interior as per website instructions. Sites that contained questionable data were not plotted.

Salinity was generated for all available data for each location from the Oceanographic Data Center from 1913 to 2010 (http://www.nodc.noaa.gov/cgi-bin/OC5/SELECT/builder.pl) and Global Temperature-Salinity Profile Program (GTSPP) from January 1990 to August 2010 (U.S. National Oceanographic Data Center, 2006) for a 16 km^2 oceanic area from all possible sample collection methods for all months. Smaller area sizes did not generate sufficient data. Only sites with data for 2 or more days were plotted.

Sea surface temperature (SST) data was generated from the Pathfinder Ver. 5.0 satellite for day and night monthly science quality composites. Monthly data was calculated in every year from September 1981 to December 2008 for all months from site coordinates. SST patterns were generated for three different size areas (8 km^2, 16 km^2 and 24 km^2) for 5 sites (02-USCABro, 06-USCASCH, 28-USCAOcc, 54-USCACCO, 66-USCABLJ) placed along the

entire site location range. No obvious pattern difference was observed so the smallest area size area was plotted.

Concentration of chlorophyll-*a* in sea water data for science quality monthly composites was generated from the Orbview-2 SeaWiFS satellite, (http://coastwatch.pfeg.noaa.gov/erddap/griddap/erdSAchlamday.html). Monthly data was calculated in every year from September 1997 to October 2006 for all months for a 16 km^2 area from all site coordinates. Area size was chosen by comparing 16 km^2 and 24 km^2, which generated similar plots when compares with each other, so the smallest size area was plotted.

Pearson's correlation coefficient for environmental data was calculated using Statistica Version 7 (www.statsoft.com, Tulsa OK, USA).

RESULTS:

The range of the North Clade (NC) is from site 01-USCACAS (43.3^{o}N) to site 38-USCAArH (34.47^{o}N), and range of the South Clade (SC) is from site 22-USCAPSN (35.73^{o}N) to site 70-MXBCPBj (29.95^{o}N) or beyond. The region where the NC and SC overlap, which is the southern limit of the NC (slNC) and the northern limit of the SC (nlSC), extends from site 22-USCAPSN to site 38-USCAArH approximately 212 km along the coast of California encompassing Point Conception (34.45^{o}N). A similar sized area was chosen at the northern limit of the North Clade (nlNC), which extends from site 01-USORCAS to approximately 200 km south encompassing site 03-USCADCD (41.65^{o}N).

Phylogeography to understand evolutionary history

Site 01-USORCAS samples were not used in the genetic diversity analysis as there were only 5 samples, but the most northern population is interesting as it showed very high or higher 16S number of alleles of 3, haplotype diversity of 0.7000 +/- 0.2184, and nucleotide diversity of 0.003704 +/- 0.002854 compared to the range of NC. In COI, there was one haplotype.

Specimen and haplotype networks

The final dataset consisted of 852 specimens from 70 locations (Fig. 2.1, Table S1). The partition-homogeneity test for concatenated 16S and COI sum of tree lengths was 34 to 47 (P value = 0.0100), with original tree length of 34, indicates that the two partitions may harbor different evolutionary information. However, analyzed in TCS, both 16S and COI haplotype networks revealed broadly similar patterns, i.e. clear genetically distinct but geographically overlapping clades.

The partial 16S gene amplicons yielded 503 nucleotides with 10 parsimony-informative characters. Alignment resulted with two gap regions, one following a polyC region consisting of 0 to 3 gaps, the other gap was a result of one position difference in one sequence. TCS networks resulted in 41 haplotypes, of which 25 were unique (Fig. 2.2a). Assessing the data separately, before and after missing and ambiguous sequences were removed, revealed no connection differences in the networks. The 16S haplotype network revealed a clear separation of the NC and SC (except for one sequence from site 53-USCAPtV) of at least 2 nucleotide differences with one unique sequence inferred as the ancestral haplotype in this separation. The NC consisted of 2 major clades (n = 315 and n = 78) with 9 unique haplotypes. The SC consisted of 3 major clades (n = 300, n = 50, n = 41) with 15 unique haplotypes.

Partial COI amplicons yielded 473 nucleotides with 13 parsimony-informative characters resulting in 35 haplotypes, of which 24 were unique. Assessing the data separately before and after missing and ambiguous sequences were removed revealed one network connection difference noted with a dotted line (Fig. 2.2b). The COI network exposed a clear separation of 2 nucleotide differences between the NC (n = 382) with 17 unique haplotypes, and the SC, which consists of 3 major clades (n = 325, n = 49, n = 39), with 8 unique haplotypes.

Abundance

Abundance, calculated as arithmetic mean of quadrat plots, ranged from 0.0 specimens per quadrat at site 03-USCADCD, within nlNC, to a mean of 62.7 specimens per quadrat at site 15-USCAFAR, which is close to the center of the range of NC. 95% Confidence Interval (CI) ranged from 0.1 to 19.1. Abundances of NC and SC were estimated by multiplying the observed abundance of all *L. scabra* by the proportion of individuals in genetic analyses that had NC vs. SC alleles and plotted against distance from site 39-USCARSB. Latitudinal variation of the NC shows a slightly skewed abundant centre distribution (Fig. 2.3).

Slatkin's linearized F_{ST}

The NC's Slatkin's linearized F_{ST} for 16S regressed on geographic distance ranged from 0.0 to 1.06667 ($y = -7x10^{-6}x + 0.022$; $R^2 = 0.00063$), and COI Slatkin's linearized F_{ST} regressed on geographic distance ranged 0.0 to 4.97619 ($y = -3x10^{-5}x + 0.1115$; $R^2 = 0.00029$). The SC's Slatkin's linearized F_{ST} for 16S vs. distance ranged from 0.0 to 11.5 ($y = 0.001x + 0.1023$; $R^2 = 0.01563$), and COI vs. distance ranged 0.0 to 29.5 ($y = 0.0005x + 0.5143$; $R^2 = 0.0009$). Slatkin's linearized F_{ST} plots showed no isolation by distance (Fig. 2.4).

Genetic diversity

Distribution and proportion of alleles and unique alleles

With the exception of site 22-USCAPSN, the NC's proportion of alleles for both 16S and COI generally decreased towards the southern limit of the NC, while the SC proportion of alleles generally decreased towards the range of the NC (Fig. 2.5a, c). The proportion of unique alleles was greater in the SC for 16S, and in the NC for COI (Fig. 2.5b, d). For the NC, the proportion of unique 16S alleles was few and somewhat evenly distributed, while the COI alleles were greater towards the nlNC (Fig. 2.5b, c). For the SC, the proportion of unique alleles was greatest in the center of its range for 16S, and few and centred for COI (Fig. 2.5b, c).

Number of alleles

Latitudinal variation for a 50 km running mean of the number of alleles (Fig. 2.6) was calculated. Number of alleles for the NC 16S ranged from 1 to 4, with the running mean from 2.0 to 4.0; and the NC COI number of alleles ranged from 1 to 5, with the running mean from 1.33 to 3.5. Number of alleles for the NC was varied throughout the range. The nlNC 16S number of alleles ranged from 2 to 4, with the running mean from 3 to 4; and the nlNC COI number of alleles ranged from 1 to 3, with the running mean from 2 to 3. The slNC 16S number of alleles ranged from 2 to 4, with the running mean from 2.8 to 3.5; and the slNC COI number of alleles ranged from 1 to 5, with the running mean from 1.5 to 2.6. The variation in the 16S running mean from the nlNC was doubled compared to the range of the NC in 16S and COI; and the variation from the range of the NC was about 3 times lower compared to the slNC in 16S, and about 2 times lower in COI.

Number of alleles for the SC 16S ranged from 1 to 7, with the running mean from 2.0 to 5.0; and the SC COI number of alleles ranged from 1 to 6, with the running mean from 1.5 to 4.0. Number of alleles for the SC increased to about 400 km from its northern range limit before decreasing towards the middle of the range, then increasing again farthest south. The number of alleles for the nlSC 16S ranged from 1 to 4, with the running mean from 2.33 to 4.25; and the nlSC COI number of alleles ranged from 2 to 3, with the running mean from 2.3 to 2.75. The variation in the running mean from the range of SC was twice that compared to the nlSC for 16S, and 6 times higher in COI.

Haplotype diversity

Latitudinal variation for a running mean of haplotype diversity (Fig. 2.7) of sites with 5 or more samples was calculated. Haplotype diversity for the NC 16S ranged from 0.0 to 0.75, with the running mean from 0.2392 to 0.697; and the NC COI haplotype diversity ranged from 0.0 to 0.4643, with the running mean from 0.67 to 0.4392. Haplotype diversity for the NC was variable throughout the range. The nlNC 16S haplotype diversity ranged from 0.2 to 0.697, with the running mean from 0.4485 to 0.697, and the nlNC COI haplotype diversity ranged from 0.0 to 0.4394, with the running mean from 0.2197 to 0.4394. The slNC 16S haplotype diversity ranged from 0.2206 to 0.6, with the running mean from 0.4099 to 0.5084, and the slNC COI haplotype diversity ranged from 0.0 to 0.4265, with the running mean from 0.0868 to 0.2157. The variation in the running mean in the range of the NC was double compared to nlNC in 16S, and only slightly higher in COI, and the variation in range of the NC was 5 times higher compared to slNC in 16S, and 3 times higher in COI.

Haplotype diversity for the SC 16S ranged from 0.0 to 0.7619, with the running mean from 0.2084 to 0.7119; SC COI haplotype diversity ranged from 0.0 to 0.7564, with the running mean from 0.0834 to 0.673. Haplotype diversity for the SC increased to about 400 km from its northern range limit before decreasing towards the middle of the range and increasing again farthest south. Haplotype diversity for nlSC 16S ranged from 0.0 to 0.7143, with the running mean from 0.3492 to 0.5572; and the nlSC COI haplotype diversity ranged from 0.3333 to 0.5238, with the running mean from 0.3700 to 0.5119. The variation in the running mean from the range of the SC was almost double compared to nlSC in 16S, and 4 times higher in COI.

Nucleotide diversity

Latitudinal variation for a running mean nucleotide diversity (Fig. 2.8) of sites with 5 or more samples was calculated. Nucleotide diversity for NC 16S nucleotide diversity ranged from 0.0 to 0.002056, with the running mean from 0.00049 to 0.002056; the NC COI nucleotide diversity ranged from 0.0 to 0.002819, with the running mean from 0.000141 to 0.000993. Nucleotide diversity for the NC was variable throughout the range. The nlNC 16S nucleotide diversity ranged from 0.000399 to 0.002056, with the running mean from 0.001228 to 0.002056; and the nlNC COI nucleotide diversity ranged from 0.0 to 0.000993, with the running mean from 0.0004965 to 0.000993. The slNC 16S nucleotide diversity ranged from 0.00044 to 0.001379, with the running mean from 0.000877 to 0.001133; and slNC COI nucleotide diversity ranged from 0.0 to 0.002819, with the running mean from 0.0001835 to 0.000901. The variation in the running mean from the range of NC was almost double compared to nlNC in 16S and COI; and the variation in the running mean from range of the NC was about 5 times higher compared to

slNC in 16S, while the range of the NC was similar to slNC in COI. Nucleotide diversity variation for the NC was somewhat stable throughout the range.

Nucleotide diversity for SC 16S ranged from 0.0 to 0.002585, with the running mean from 0.000416 to 0.002414; and the SC COI nucleotide diversity ranged from 0.0 to 0.004309, with the running mean from 0.000353 to 0.003470. Nucleotide diversity for the SC increased to about 400 km from its northern range limit before decreasing towards the middle of the range, then increasing again farthest south. The variation in the running mean in the range of the NC was almost 5 times higher compared to slNC in 16S and COI.

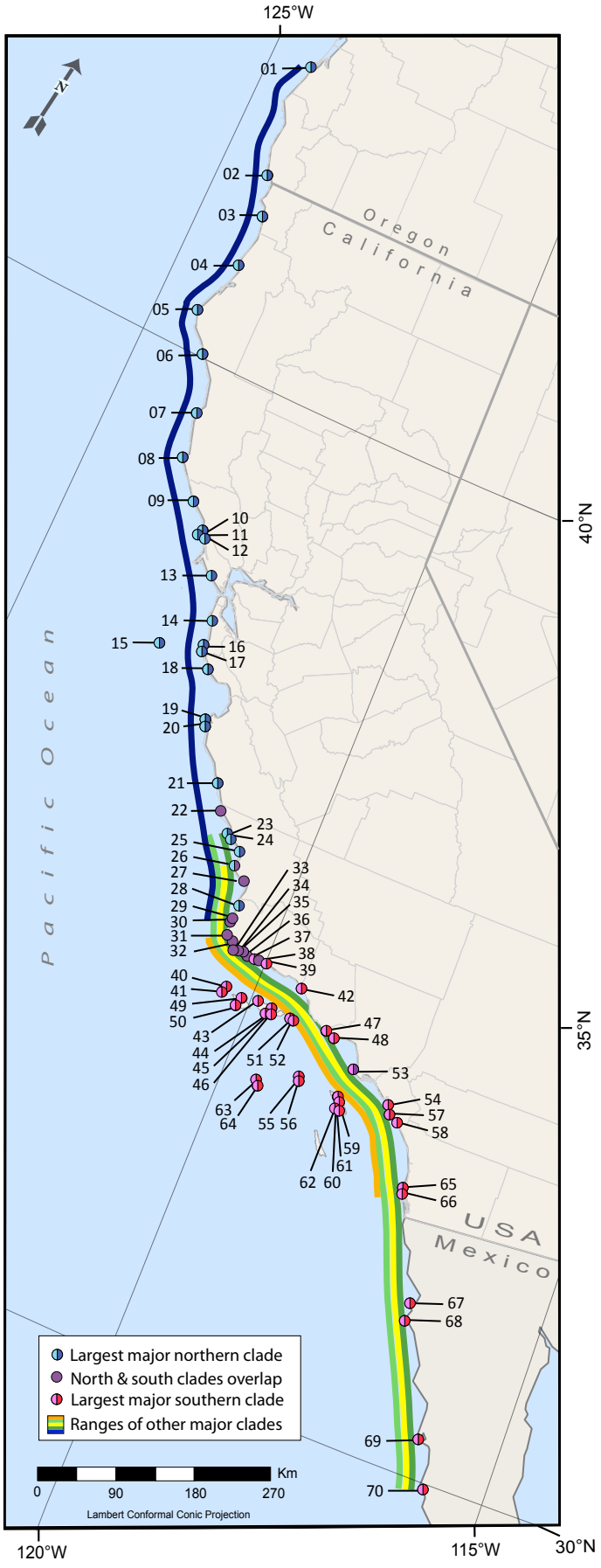

Figure 2.1: Map of the west coast of North America from southern Oregon, USA, to Baja California, Mexico, showing site locations of *Lottia scabra*. Numbers are site locations (Fig. 2 and Table S1). Blue/light blue circles indicate the sites from which the largest major northern clade for both 16S and COI was collected; red/magenta circles indicate the sites from which the largest major southern clade for both 16S and COI was collected; purple circles show sites that have both northern and southern major clades. Colored lines show the ranges of other major clades on the 16S and COI haplotype networks (Fig. 2.2).

Figure 2.2: Haplotype networks for *Lottia scabra* (a) 16S and (b) COI. Each branch length indicates one nucleotide difference. Each circle or square represents a sampled (colored) or inferred but unsampled (colorless) allele; numbers correspond to site locations (Fig. 2.1 and Table S1). The area of each circle or square is proportional to the frequency with which that haplotype was sampled (see scales). Color fills represent the geographic regions from which haplotypes were collected, and the area of each color is also proportional to frequency. Blue/light blue colors indicate sites with only the northern clade, red/magenta colors represent sites with only the southern clade, and purple represents sites at which both the northern and southern clades were sampled. (a) 16S haplotype network shows 41 haplotypes, including 2 major northern alleles (blue ring, n = 315; dark blue ring, n = 78) and 3 major southern clades (red ring, n = 300; orange ring, n = 50; green ring, n = 41). Square shows inferred ancestral haplotype (n = 1). (b) COI haplotype network shows 35 haplotypes including one major northern allele (light blue ring, n = 382) and 3 major southern alleles (pink ring, n = 325; yellow ring, n = 49; and light green ring, n = 39). Dotted line shows alternate connection from separate analysis before missing and ambiguous positions were removed.

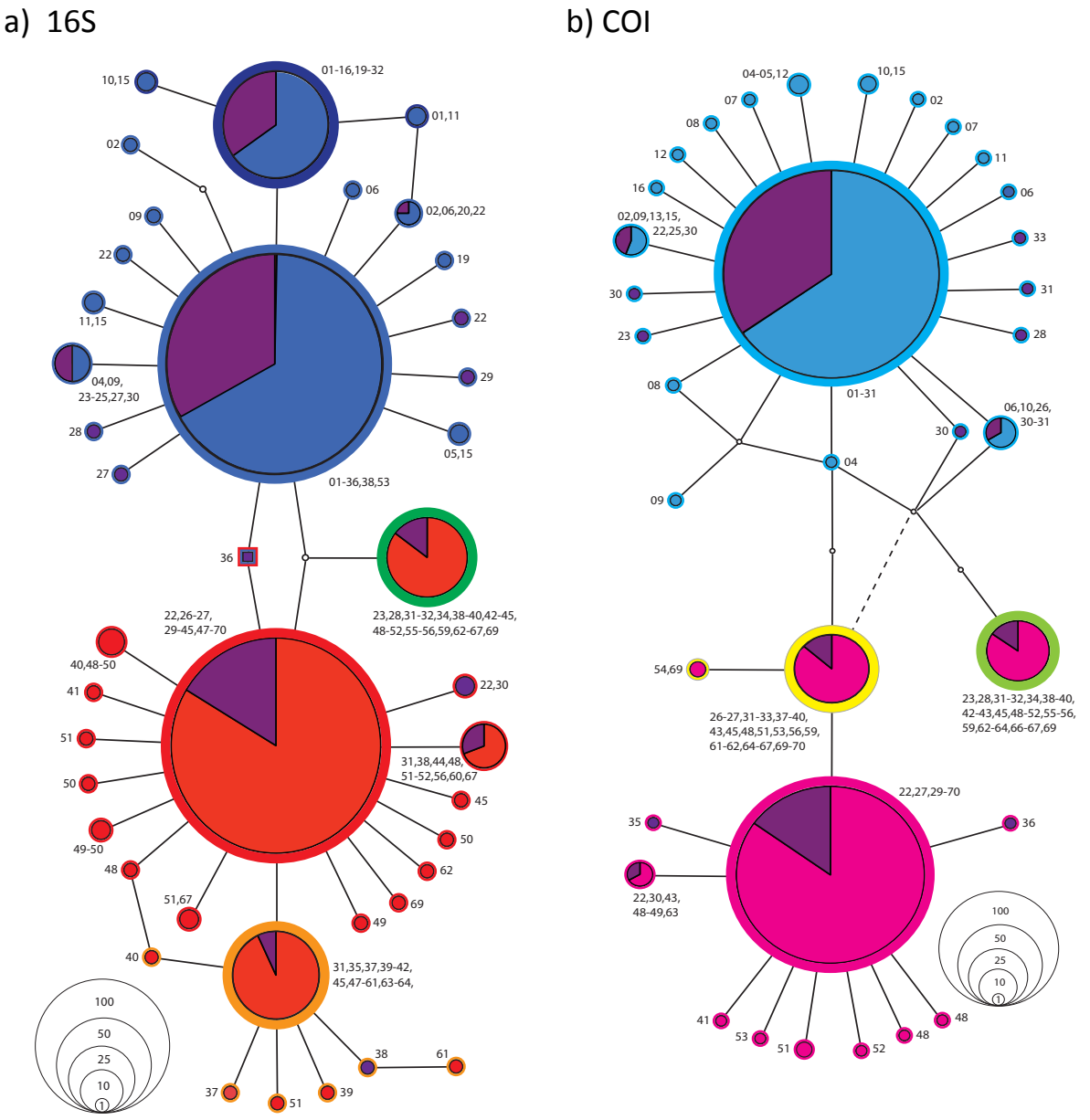

Figure 2.3: Abundance of *Lottia scabra* (mean +/- 95% C.I.) west and north of 39-USCARSB (from Coastal Biodiversity Surveys, http://cbsurveys.ucsc.edu). Abundances of North Clade (x) and South Clade (o) estimated by multiplying the observed abundance of all *L. scabra* by the proportion of individuals in genetic analyses that had North vs. South alleles. Mean abundance ranged from 0.0 specimens/quadrat (at 03-USCADCD) to 62.7 specimens/quadrat (at 15-USCAFAR). Shaded areas represent the northern limit northern limit of the North Clade, which is from 01-USORCAS (43.31°N) to 03-USCADCD (41.65°N) and the southern limit of the North Clade from 22-USCAPSN (35.73°N) to 38-USCAArH (34.47°N). *L. scabra* shows a slightly skewed abundant centre distribution for the North Clade.

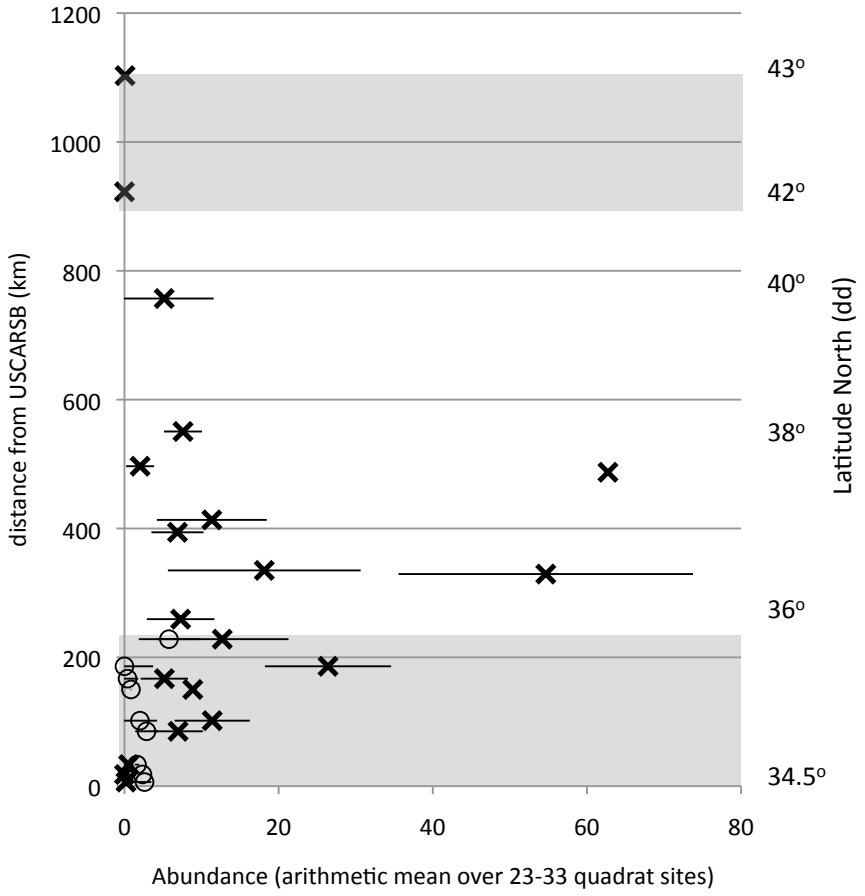

Figure 2.4: Slatkin's Linearized F_{ST} for *Lottia scabra* as log distance for all combinations of sites. 16S filled circles and solid trendline, COI open squares and dashed trendline, (a) North Clade: 16S F_{ST} 0.0 to 1.06667, log distance km range -0.35 to 3.04, trendline y = -0.0011x + 0.022, $R^2 = 5.1x10^{-5}$; COI F_{ST} 0.0 to 4.97619, log distance km range -0.35 to 2.97, trendline y = -0.0074x + 0.1188, $R^2 = 7x10^{-5}$. (b) South Clade: 16S F_{ST} 0.0 to 11.5, log distance km range 0.05 to 2.88, trendline y = 0.3414x - 0.4468, R^2 = 0.01563; COI F_{ST} 0 to 29.5. log distance 0.05 to 2.88, trendline y = 0.3171x - 0.0653, R^2 = 0.00278. Plots show no isolation by distance.

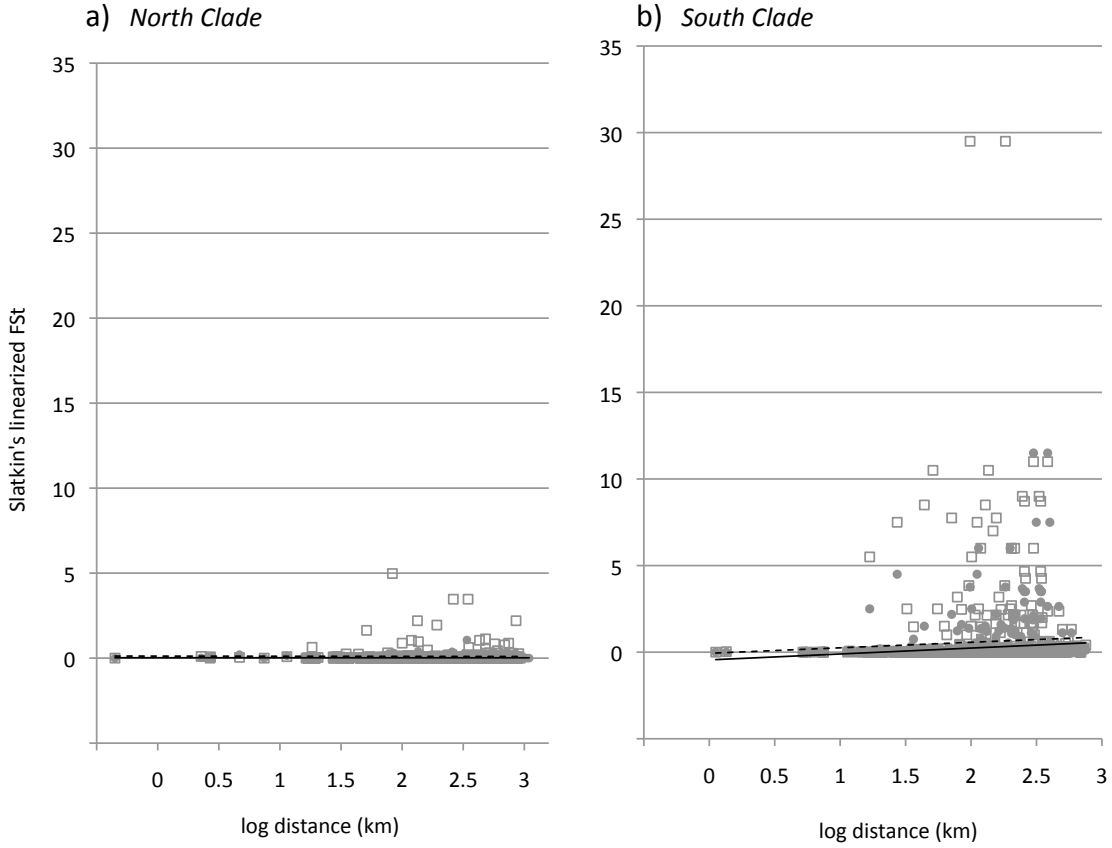

Figure 2.5: Proportion of alleles and unique alleles per site for *Lottia scabra.* Colors correspond to Figs. 2.1 and 2.2 (a) Proportion of 16S alleles per site, (b) Proportion of unique 16S alleles per site, (c) Proportion of COI alleles per site, (d) Proportion of unique COI per site. The North Clade's proportion of alleles for both 16S and COI generally decreases towards southern limit North Clade, while the South Clade's proportion generally decreases towards northern limit South Clade (a, c). Unique 16S alleles for the North Clade are few and evenly distributed, while the South Clade shows a greater number with most towards the center of the range (b). Unique COI alleles for the North Clade shows alleles greatest towards northern limit North Clade, while for the South Clade they are few and centered in the range (d).

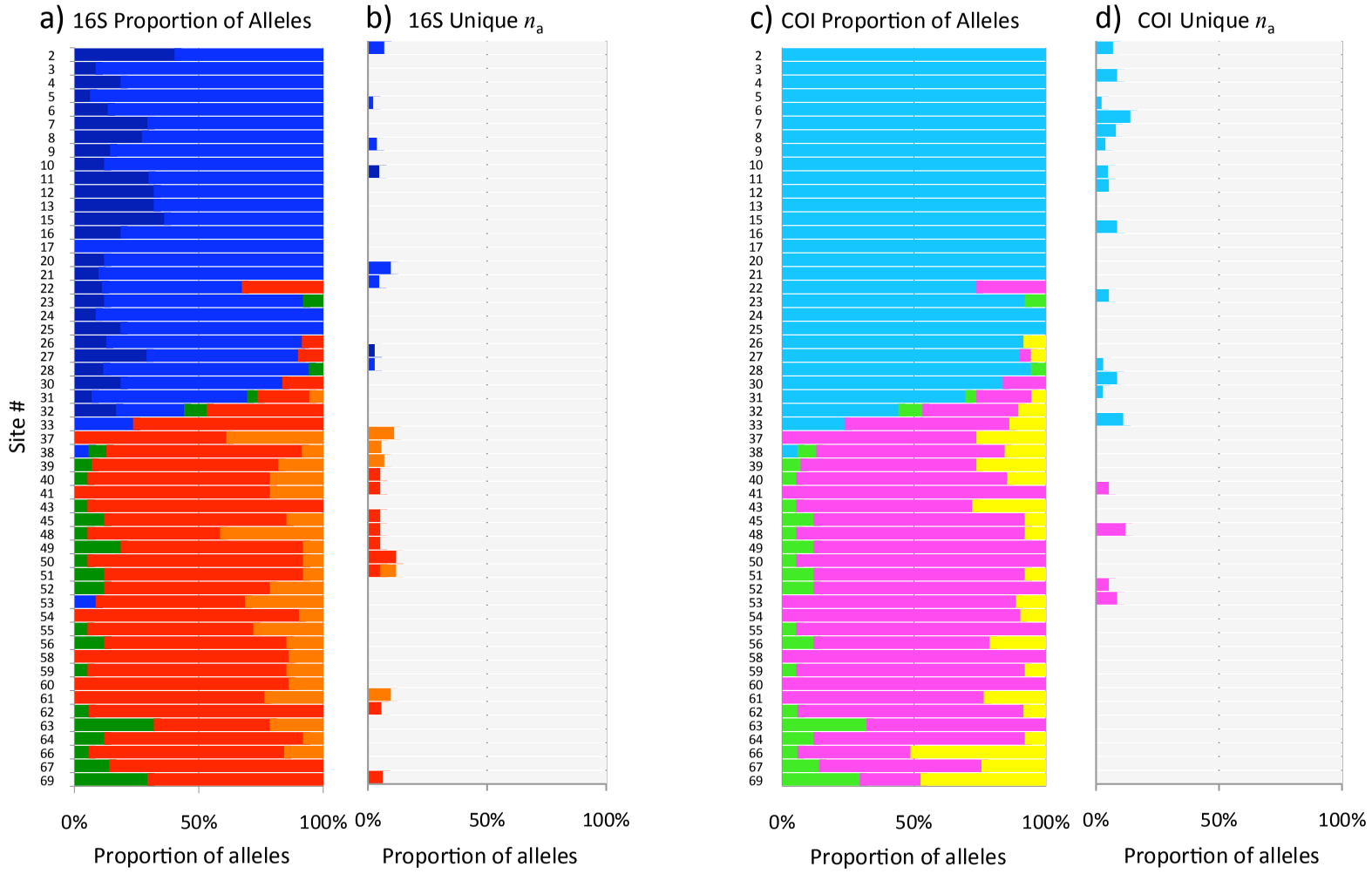

Figure 2.6: Latitudinal variation for running mean of the number of alleles for *Lottia scabra* of sites with 5 or more samples. 16S filled circles, COI open squares. (a) Running mean number of alleles of the North Clade, distance from the southern range limit of the North Clade (38-USCAArH at 34.5°N). Number of alleles for the North Clade 16S ranged from 1 to 4, mean from 2.0 to 4.0; and COI from 1 to 5, mean from 1.33 to 3.5. (b) Running mean number of alleles of the South Clade, distance of the northern range limit of the South Clade (22-USCAPSN at 35.7°N). Number of alleles for the South Clade 16S was 1 to 7, mean from 2.0 to 5.0; and COI from 1 to 6, mean from 1.5 to 4.0. Black points indicate mean of 2+ sites, gray points indicate 1 site. Shaded areas represent the northern limit of the North Clade, which is from 03-USCADCD (41.65°N) to 01-USORCAS (43.31°N, ~100 km north of graph, not shown), and the southern limit of the North Clade 22-USCAPSN (35.73°N) to 38-USCAArH (34.47°N).

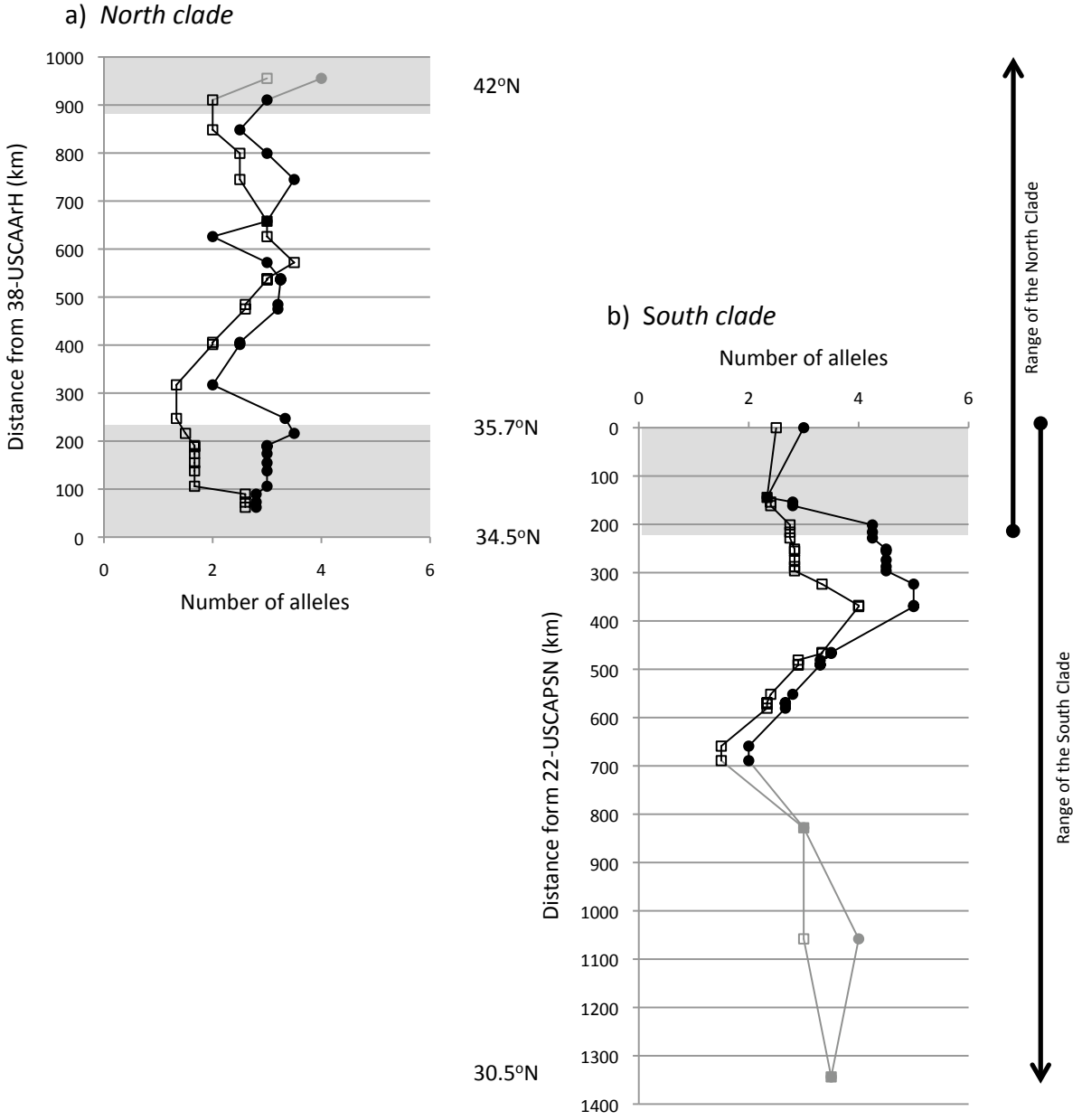

Figure 2.7: Latitudinal variation for running mean haplotype diversity for *Lottia scabra* of sites with 5 or more samples. 16S filled circles, COI open squares. (a) Running mean haplotype diversity of the North Clade, distance from the southern limit of the North Clade (38-USCAArH at 34.5°N). Haplotype diversity for the North Clade for 16S was 0.0 to 0.75, mean was 0.239 to 0.697; and COI was 0.0 to 0.464, mean was 0.67 to 0.439. (b) Running mean haplotype diversity for the South Clade, distance of the northern range limit of the South Clade (22-USCAPSN at 35.7°N). Haplotype diversity for 16S was 0.0 to 0.762, mean from 0.208 to 0.712; COI from 0.0 to 0.756, mean from 0.083 to 0.673. Black points indicate mean of 2+ sites, gray points indicate 1 site. Shaded areas represent the northern limit of the North Clade, which is from 03-USCADCD (41.65°N) to 01-USORCAS (43.31°N, ~100 km north of graph, not shown), and the southern limit of the North Clade 22-USCAPSN (35.73°N) to 38-USCAArH (34.47°N).

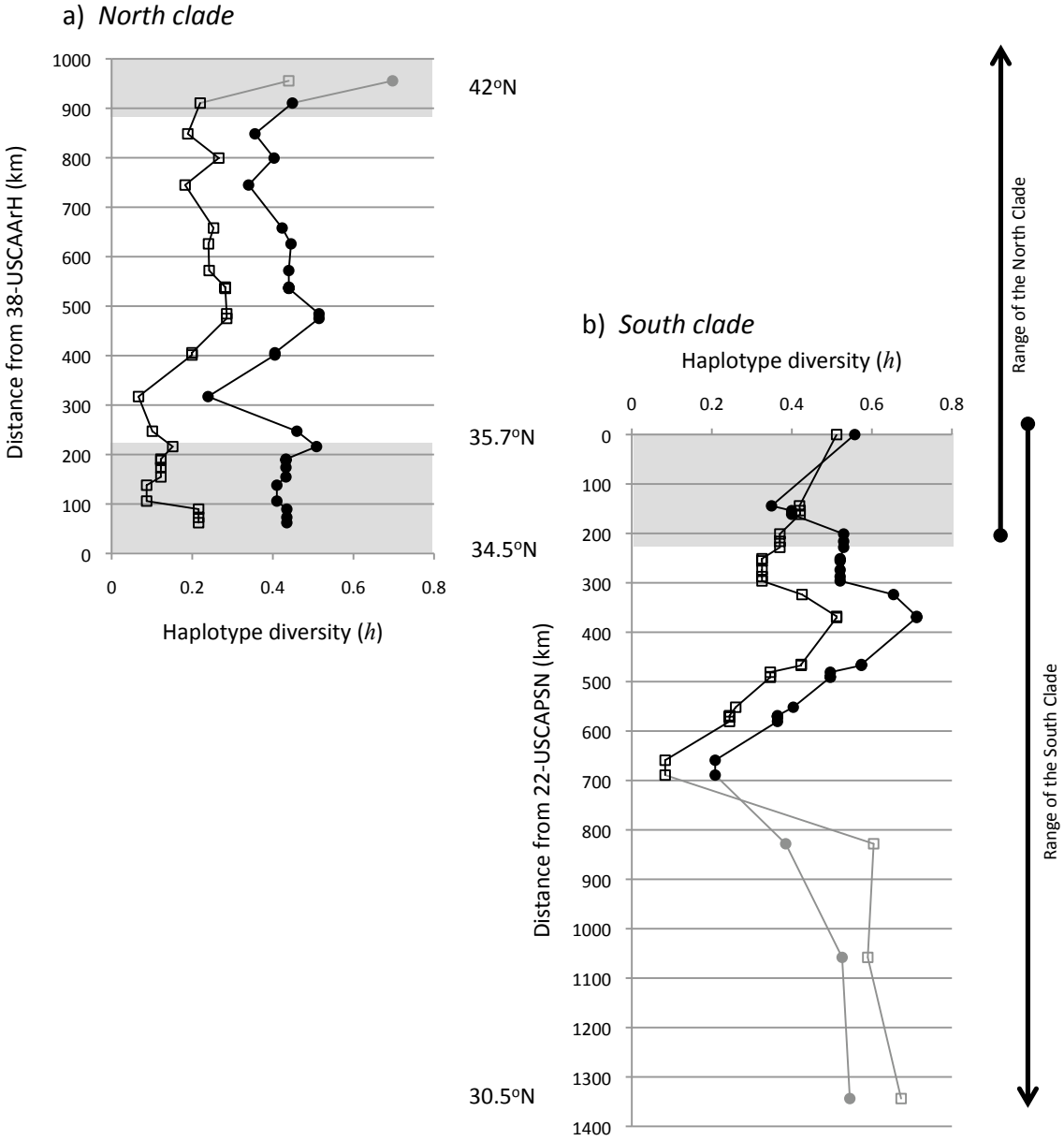

Figure 2.8: Latitudinal variation for running mean nucleotide diversity for *Lottia scabra* of sites with 5 or more samples. 16S filled circles, COI open squares. (a) Running mean nucleotide diversity of the North Clade, distance from the southern limit of the North Clade (38-USCAArH at 34.5°N). Nucleotide diversity for 16S from 0.0 to 0.002056, mean from 0.00049 to 0.002056; COI from 0.0 to 0.002819, mean from 0.000141 to 0.000993. (b) Running mean nucleotide diversity of the South Clade, distance from the northern range limit of the South Clade (22-USCAPSN at 35.7°N). Nucleotide diversity for 16S 0.0 to 0.002585, mean from 0.000416 to 0.002414; COI from 0.0 to 0.004309, mean from 0.000353 to 0.003470. Black points indicate mean of 2+ sites, gray points indicate 1 site. Shaded areas represent the northern limit of the North Clade, which is from 03-USCADCD (41.65°N) to 01-USORCAS (43.31°N, ~100 km north of graph, not shown), and the southern limit of the North Clade 22-USCAPSN (35.73°N) to 38-USCAArH (34.47°N).

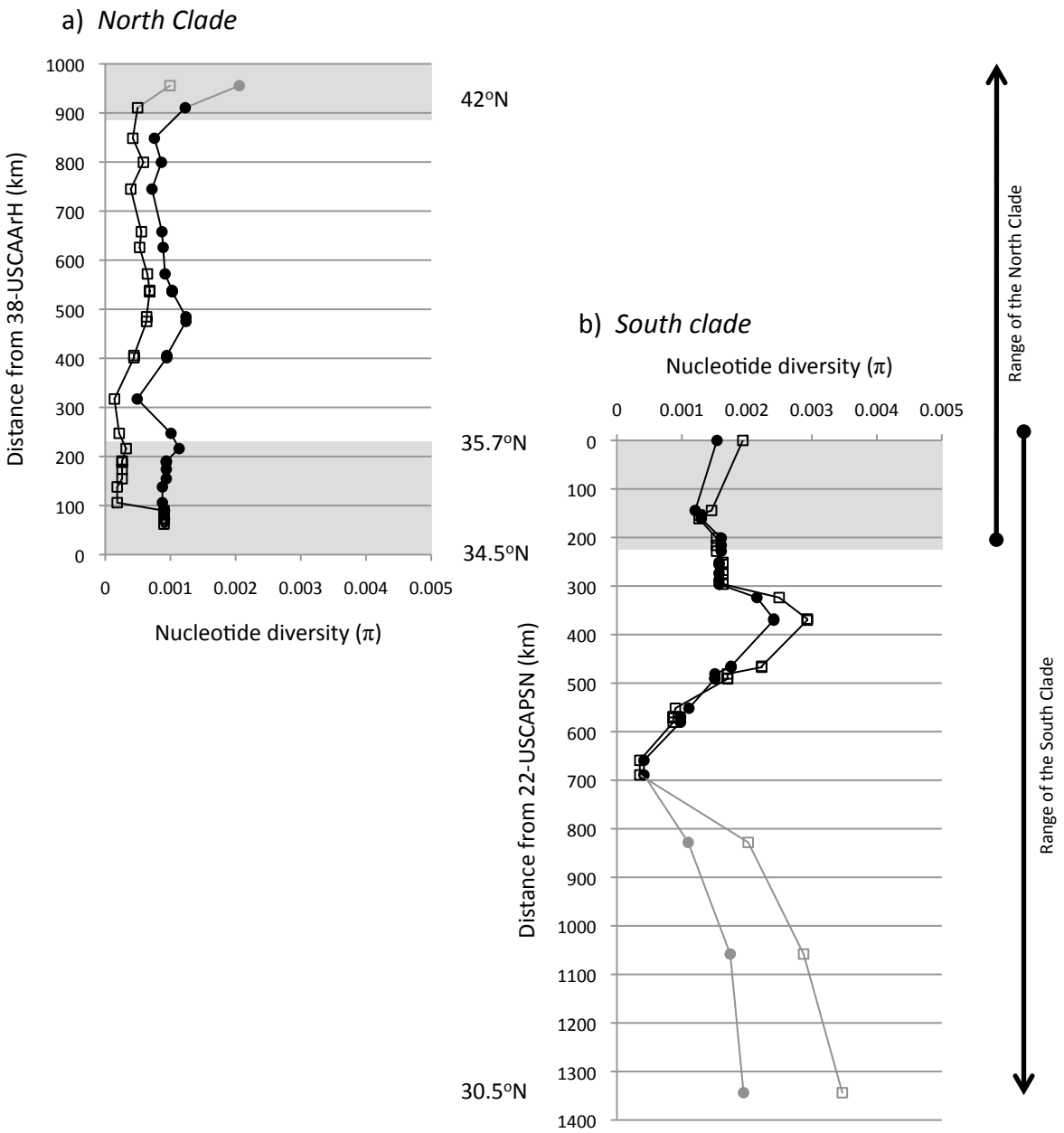

Environmental pattern

Environmental conditions values are found in Table S3.

Air temperature

Latitudinal variation of air temperature was averaged monthly (Fig. 2.9). June temperature ranged from 11.08 to 25.58 ^{o}C, with a median of 18.07 ^{o}C, and December ranged from 5.38^{o}C to 21.50^{o}C, with a median of 14.26^{o}C. June air temperature was highly positively correlated (P = 0.000) with air temperature in July (r = 0.9704) and August (r = 0.9574). December was highly positively correlated with air temperature in January (r = 0.9989), February (r = 0.9863), and November (r = 0.9909). In June, air temperature varied throughout both ranges, but mostly decreased from north to south in the slNC. In December, air temperature increased steadily from north to south towards the center of the range of SC where it became more varied. Comparison of the air temperature intensity in the range of the NC was slightly higher compared to nlNC in June and December, and variation in the range of the NC was more than 4 times higher than in nlNC in June, and 3 times in December. Comparison of the air temperature in the range of the NC was about the same intensity compared to slNC in June, and slightly higher in slNC compared to the range of the NC in December. The variation of air temperature in the range of the NC was slightly higher compared to slNC in June, and almost 2 times higher in December. The air temperature in the slNC was about the same as in the range of the SC, and variation slightly increased in June and December.

Daily total precipitation

Latitudinal variation for precipitation was averaged monthly (Fig. 2.10). Precipitation for June

ranged from 0.0 to 0.557 cm/day, with a median of 0.0 cm/day; and December ranged from 0.0 to 2.71 cm/day, with a median of 0.258 cm/day. December precipitation was highly correlated (P = 0.000) with precipitation in January (r = 0.9814), April (r = 0.9864), May (r = 0.9951), August (r = 0.9633), October (r = 0.9934), and November (r = 0.9935). In June, precipitation was low at the nlNC then decreased from north to south to almost zero throughout the remainder of all ranges. In December, precipitation was highest and most varied at the nlNC and decreased steadily from north to south throughout the ranges becoming more varied in the center of the range of the SC. Precipitation in the nlNC was almost 5 times higher compared to the range of the NC, and variation was about the same in June. Precipitation in the nlNC was almost 2 times higher compared to the range of the NC, and variation was about the same in December. The precipitation in range of the NC was about 6 times higher compared to slNC, and variation was 7 times higher in June. Precipitation in the range of the NC was 5 times higher compared to the slNC, and variation was 7 times higher in December. Precipitation and variation in the range of NC and slNC was similar in June. The precipitation in the range of the NC was 2 times higher compared to slNC, and variation was more than 2.5 times higher in December. The precipitation in the slNC was similar to the range of the SC in June and December, and variation was almost doubled in the slNC in June and increased slightly in December.

Vapor pressure deficit

Latitudinal variation for vapor pressure deficit was averaged monthly (Fig. 2.11). Vapor pressure deficit for June ranged from 75.805 to 2538.468 Pa, with a median of 1364.206 Pa; and December ranged from 285.51 to 2209.935 Pa, with a median of 775.893 Pa. June VPD was highly correlated (P = 0.000) with VPD in May (r = 0.9586). December was highly correlated (P

= 0.000) with VPD in January (r = 0.9985), February (r = 0.9949), and November (r = 0.9912). In June, the vapor pressure deficit increased somewhat steadily from north to south from the nlNC through most of the range of the NC, then it decreased across the slNC, where it became varied in the range of the SC. In December, the vapor pressure deficit increased steadily from north to south towards the slNC, where variation increased somewhat and became more varied in the center of the range of the SC. The VPD in range of the NC was about 2 times higher, and variation was more than 4 times higher in June, than in the nlNC. The VPD in range of the NC was about 2 times higher, and variation more than 8 times higher in December, than in the nlNC. The VPD intensity and variation was similar in the range of the NC and the slNC in June and December. The VPD intensity and variation was similar in the slNC and the range of the SC in June and December.

Total daily incident shortwave flux

Latitudinal variation was calculated for total daily incident shortwave flux (Fig. 2.12). Total daily incident shortwave flux for June ranged from 1907.66 to 6983.82 Wm^{-2}*daylength, with a median of 3428.67 Wm^{-2}*daylength; and December ranged from 1067.44 to 2812.19 Wm^{-2}*daylength, with a median of 2169.21 Wm^{-2}*daylength. June solar radiation was highly correlated (P = 0.000) with solar radiation in August (r = 0.9614). December solar radiation was highly correlated (P = 0.000) with solar radiation in January (r = 0.9921), February (r = 0.9772), October (r = 0.9828), and November (r = 0.9993). In June, solar radiation increased steadily and variation decreased from north to south throughout the ranges towards the center of the range of the SC where variation increased somewhat. In December, solar radiation increased steadily from north to south throughout the ranges. The solar radiation variation was similar in the nlNC

and the range of the NC then decreased towards the slNC and became more varied in the range of the SC in June. The solar radiation variation in the range of the NC was about 3 times higher compared to nlNC and slNC and about 1.5 times higher compared in the range of the SC in December.

Salinity

Latitudinal variation was calculated for salinity averaged monthly (Fig. 2.13). Salinity for May-July ranged from 30.844 to 34.067 PPS, with a median of 33.627 PPS; and November-January ranged from 28.648 to 33.941 PPS, with a median of 33.484 PPS. In the months of May-July, from north to south salinity was varied in the range of the NC, but variation decreased at slNC, before it became more varied again in the centre of the range of the SC. In November-January, from north to south, salinity increased towards the slNC, with most variation in the center of the range of the NC. There was no salinity average for the nlNC because of only one sample site. The variation in the range of the NC was 4 times higher compared to slNC in May-July and almost 2 times higher in November-January. The variation in the range of the SC was slightly higher compared to the slNC in May-July and November-January.

Sea surface temperature

Latitudinal variation was calculated for SST (Fig. 2.14). SST for June ranged from 8.713 ^{o}C to 20.625 ^{o}C, with a median of 13.704 ^{o}C; and December ranged from 9.0 ^{o}C to 19.53 ^{o}C with a median of 14.038 ^{o}C. June SST was highly correlated ($P = 0.000$) with SST in March ($r = 0.9836$), April ($r = 0.9889$), May ($r = 0.994$), July ($r = 0.9732$), August ($r = 0.9798$), September ($r = 0.9769$), and October ($r = 0.9735$). December SST was highly correlated with SST in

January (r = 0.9964), February (r = 0.9945), March (r = 0.9585), July (r = 0.9788), August (r = 0.9598), September (r = 0.9673), October (r = 0.98130), and November (r = 0.9937). In June, from north to south SST was lowest in the northern half of the range of the NC then increased towards the range of the SC. SST intensity in the range of the NC increased over 2^{o}C compared to the nlNC, and increased over 1^{o}C from the range of the NC to slNC, and 1^{o}C from slNC to the range of the SC in December. SST intensity and variation greatly increased south of the slNC becoming warm and less varied in the most southern part of the range of the SC. In December, from north to south SST increased steadily through the slNC, then in the range of the SC intensity greatly increased towards the center of the range of the SC. In June, the range of the SC became almost 2^{o}C warmer on average compared to the slNC. The variation of SST was slightly higher in the range of the NC compared to the nlNC and slNC, and variation was similar in the range of the SC compared to the slNC in June and December.

Chlorophyll a

Latitudinal variation was calculated for monthly composites of concentration of chlorophyll-*a* in sea water (Fig. 2.15). Concentration of chlorophyll-*a* in sea water for June ranged from 0.236 to 9.821 mg m^{-3}, with a median of 1.904 mg m^{-3}; and December ranged from 0.247 to 4.795 mg m^{-3}, with a median of 1.142 mg m^{-3}. In June, from north to south chlorophyll-*a* was variable in the range of the NC before intensity and variation decreased south of the slNC, then intensity and variation increased again towards the most southern site. In December, from north to south chlorophyll-*a* was variable in the range of the NC and intensity and variation decreased south of the slNC before intensity increased slightly at the most southern site. The chlorophyll-*a* in the nlNC was almost 1.5 times higher compared to the range of the NC in June and December, and

variation was similar in June, but almost 2 times higher in December. The chlorophyll-*a* decreases steadily throughout the ranges from north to south in June and December where in the range of the SC it became about 1.5 times lower compared to the slNC. The variation chlorophyll-*a* in the slNC and range of the SC are similar, and slightly lower then the range of the NC in December.

Figure 2.9: Latitudinal variation for air temperature averaged monthly for *Lottia scabra* sites for June and December taken daily from 1980 to 2003 when available from Daymet (http://www.daymet.org). June temperature was 11.082 to 25.584 °C, with a median of 18.065, and December was 5.378°C to 21.503°C, with a median of 14.259°C. Error bars represent minimum and maximum temperatures. Shaded areas represent the nlNC, which is from 03-USCADCD (41.65°N) and extends north to 01-USORCAS (43.31°N, ~100 km north of graph, not shown), and the slNC from 22-USCAPSN (35.73°N) to 38-USCAArH (34.47°N).

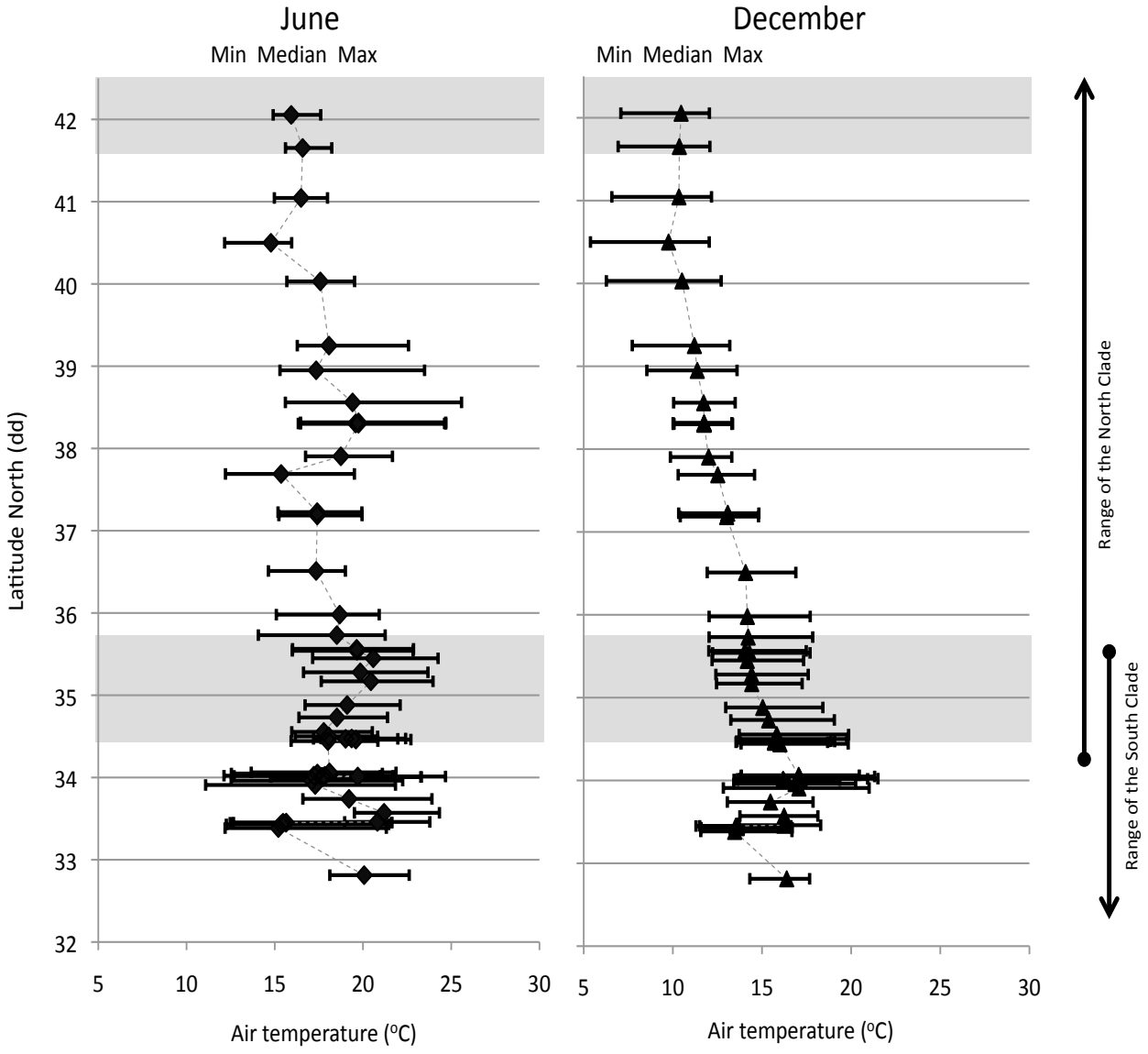

Figure 2.10: Latitudinal variation for precipitation averaged monthly for *Lottia scabra* sites for June and December taken daily from 1980 to 2003 when available from Daymet. Precipitation range for June was 0.0 to 0.557 cm/day, with a median of 0.0 cm/day; and December was 0.0 to 2.71 cm/day, with a median of 0.258 cm/day (http://www.daymet.org). Error bars represent minimum and maximum precipitation. Shaded areas represent the nlNC, which is from 03-USCADCD (41.65°N) and extends north to 01-USORCAS (43.31°N, ~100 km north of graph, not shown), and the slNC from 22-USCAPSN (35.73°N) to 38-USCAArH (34.47°N).

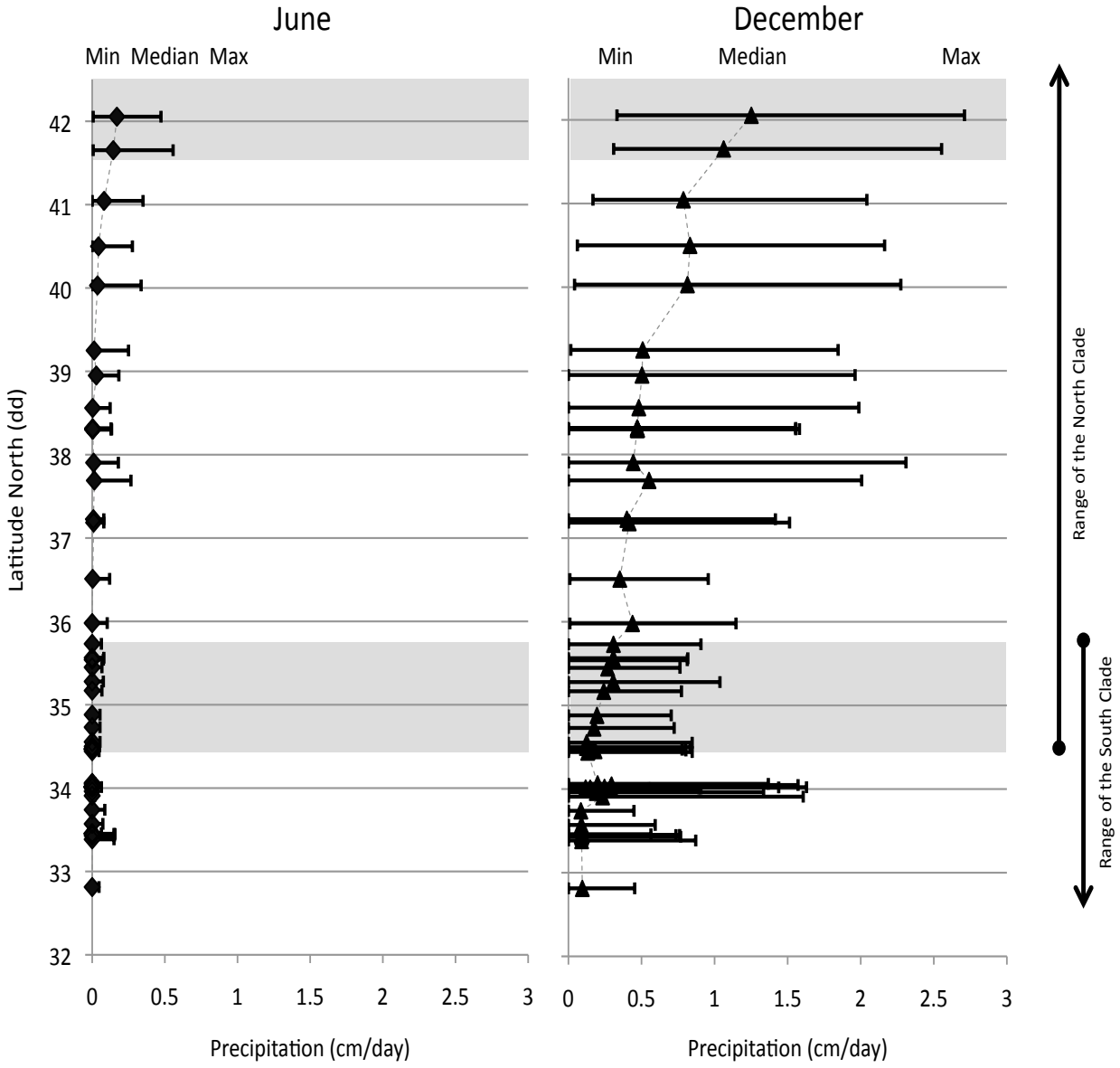

Figure 2.11: Latitudinal variation for vapor pressure deficit averaged monthly for *Lottia scabra* sites for June and December taken daily from 1980 to 2003 when available from Daymet (http://www.daymet.org). Vapor pressure deficit range for June was 75.805 to 2538.468 Pa, with a median of 1364.206 Pa; and December was 285.51 to 2209.935 Pa, with a median of 775.893 Pa. Error bars represent minimum and maximum VPD. Shaded areas represent the nlNC, which is from 03-USCADCD (41.65°N) and extends north to 01-USORCAS (43.31°N, ~100 km north of graph, not shown), and the slNC from 22-USCAPSN (35.73°N) to 38-USCAArH (34.47°N).

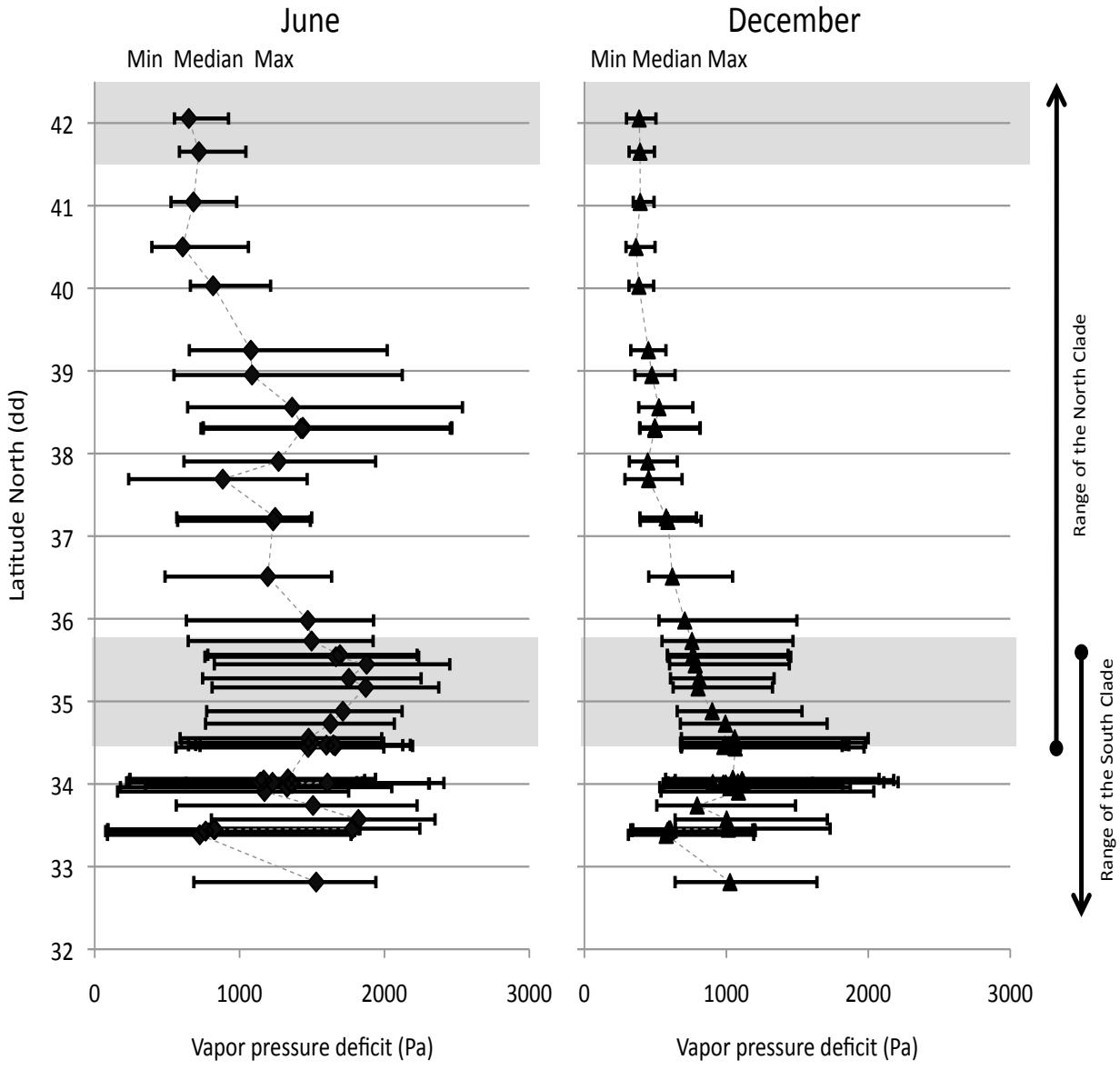

Figure 2.12: Latitudinal variation for total daily incident shortwave flux averaged monthly for *Lottia scabra* sites for June and December taken daily from 1980 to 2003 when available from Daymet (http://www.daymet.org). Total daily incident shortwave flux range for June was 1907.664 to 6983.817 Wm^{-2}*daylength, with a median of 3428.673 Wm^{-2}*daylength; and December was 1067.435 to 2812.190 Wm^{-2}*daylength, with a median of 2169.208 Wm^{-2}*daylength. Error bars represent minimum and maximum temperatures. Shaded areas represent the nlNC, which is from 03-USCADCD (41.65°N) and extends north to 01-USORCAS (43.31°N, ~100 km north of graph, not shown), and the slNC from 22-USCAPSN (35.73°N) to 38-USCAArH (34.47°N).

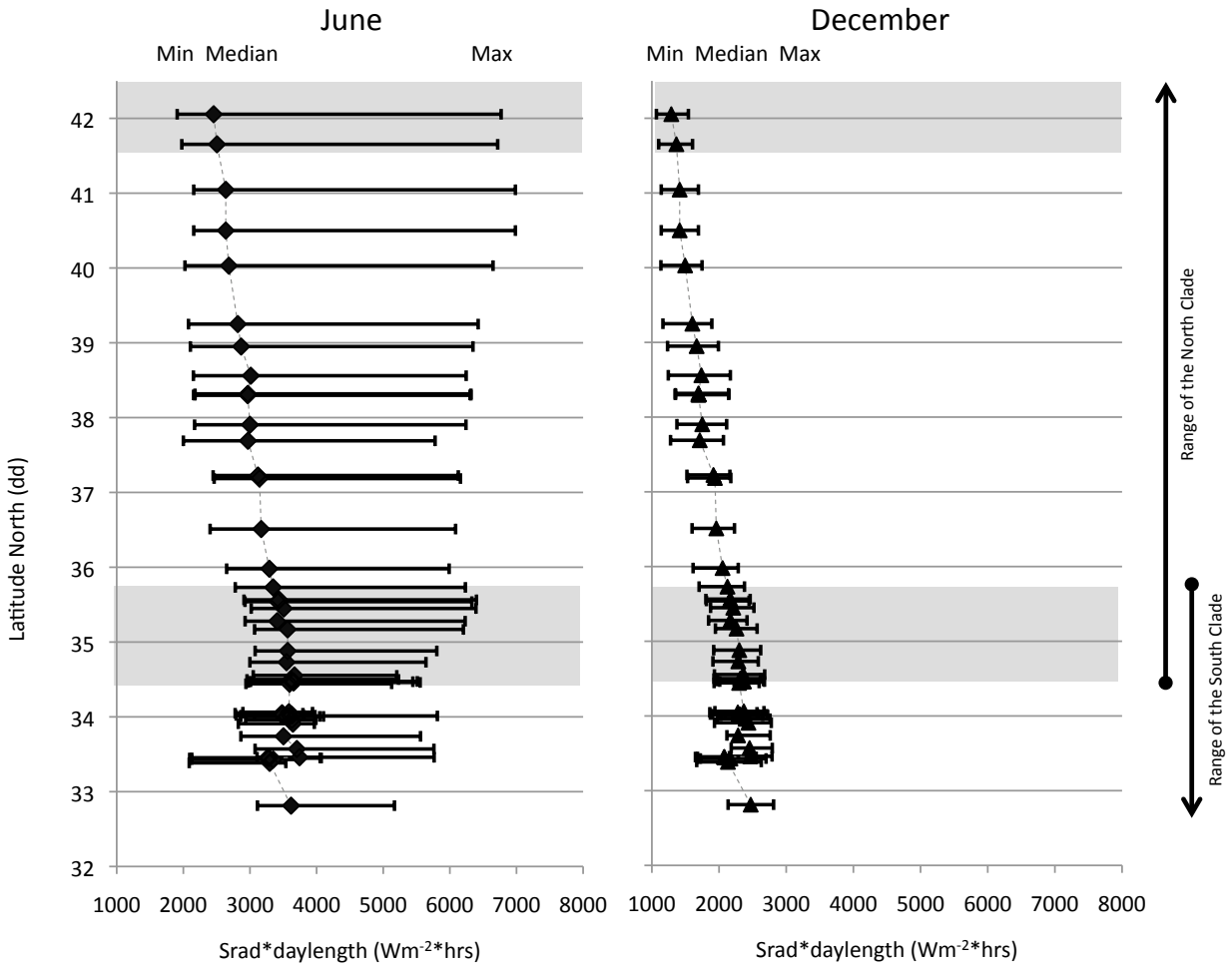

Figure 2.13: Latitudinal variation for salinity averaged monthly for *Lottia scabra* sites for composite of monthly averages as a proxy for June and December taken daily from 1913 to 2010 when available from National Oceanographic Data Center (2006) and http://www.nodc.noaa.gov/cgi-bin/OC5/SELECT/builder.pl. Salinity range for May-June-July was 30.8435 to 34.067 PPS, with a median of 33.627 PPS; and November-December-January was 28.648 to 33.941 PPS, with a median of 33.484 PPS. Error bars represent minimum and maximum salinity. Shaded areas represent the nlNC, which is from 03-USCADCD (41.65°N) and extends north to 01-USORCAS (43.31°N, ~100 km north of graph, not shown), and the slNC from 22-USCAPSN (35.73°N) to 38-USCAArH (34.47°N).

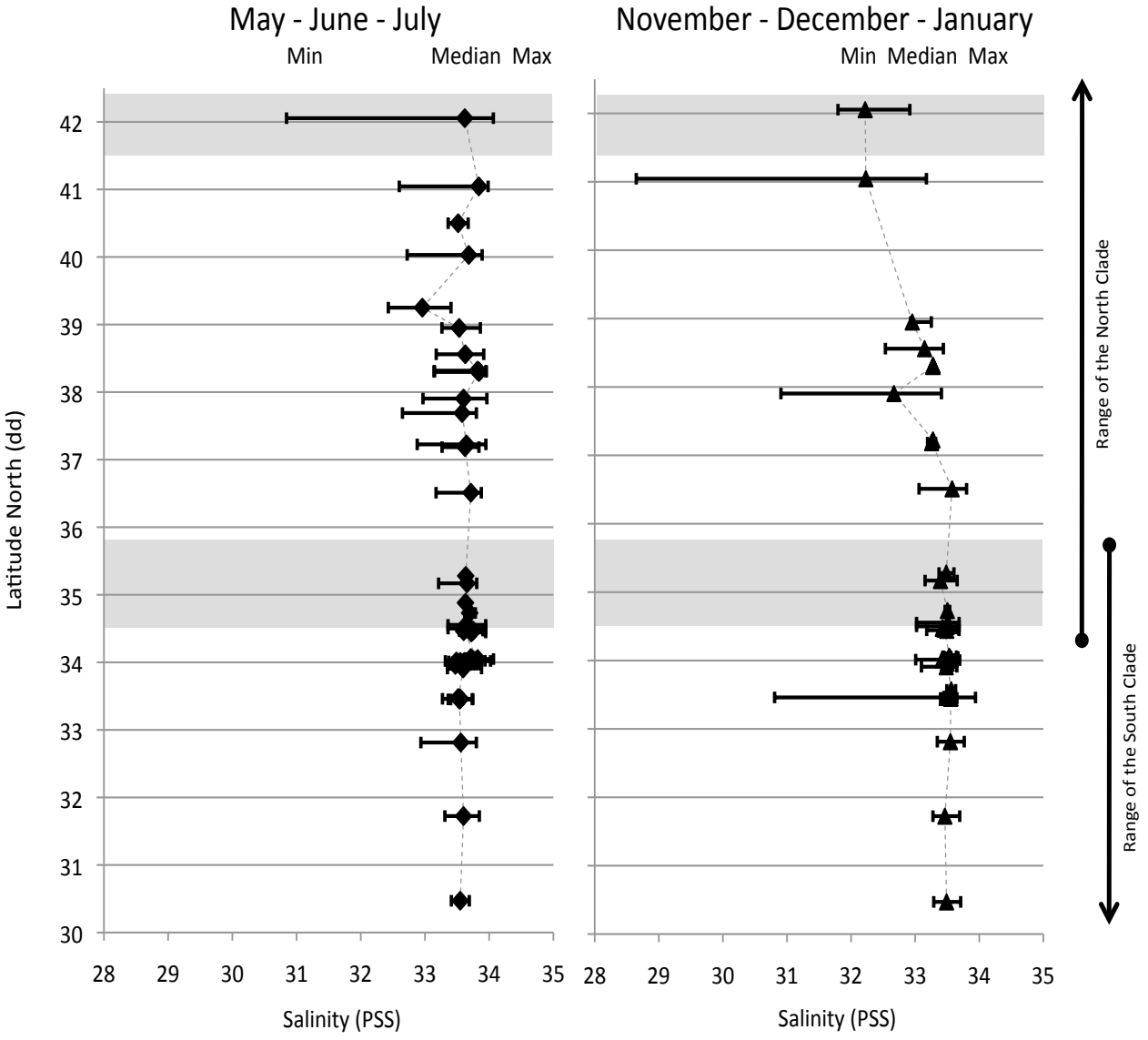

Figure 2.14: Latitudinal variation for sea surface temperature (SST) monthly composites for *Lottia* scabra sites for June and December from 1981 to 2008 from NOAA Coastwatch (http://coastwatch.pfeg.noaa.gov/erddap/griddap/erdPHsstamday.html). SST range for June 8.713 ^{o}C to 20.625 ^{o}C with a median of 13.704 ^{o}C; and December was 9.0 ^{o}C to 19.53 ^{o}C with a median of 14.038 ^{o}C. Error bars represent minimum and maximum temperatures. Shaded areas represent the nlNC, which is from 03-USCADCD (41.65^{o}N) and extends north to 01-USORCAS (43.31^{o}N, ~100 km north of graph, not shown), and the slNC from 22-USCAPSN (35.73^{o}N) to 38-USCAArH (34.47^{o}N).

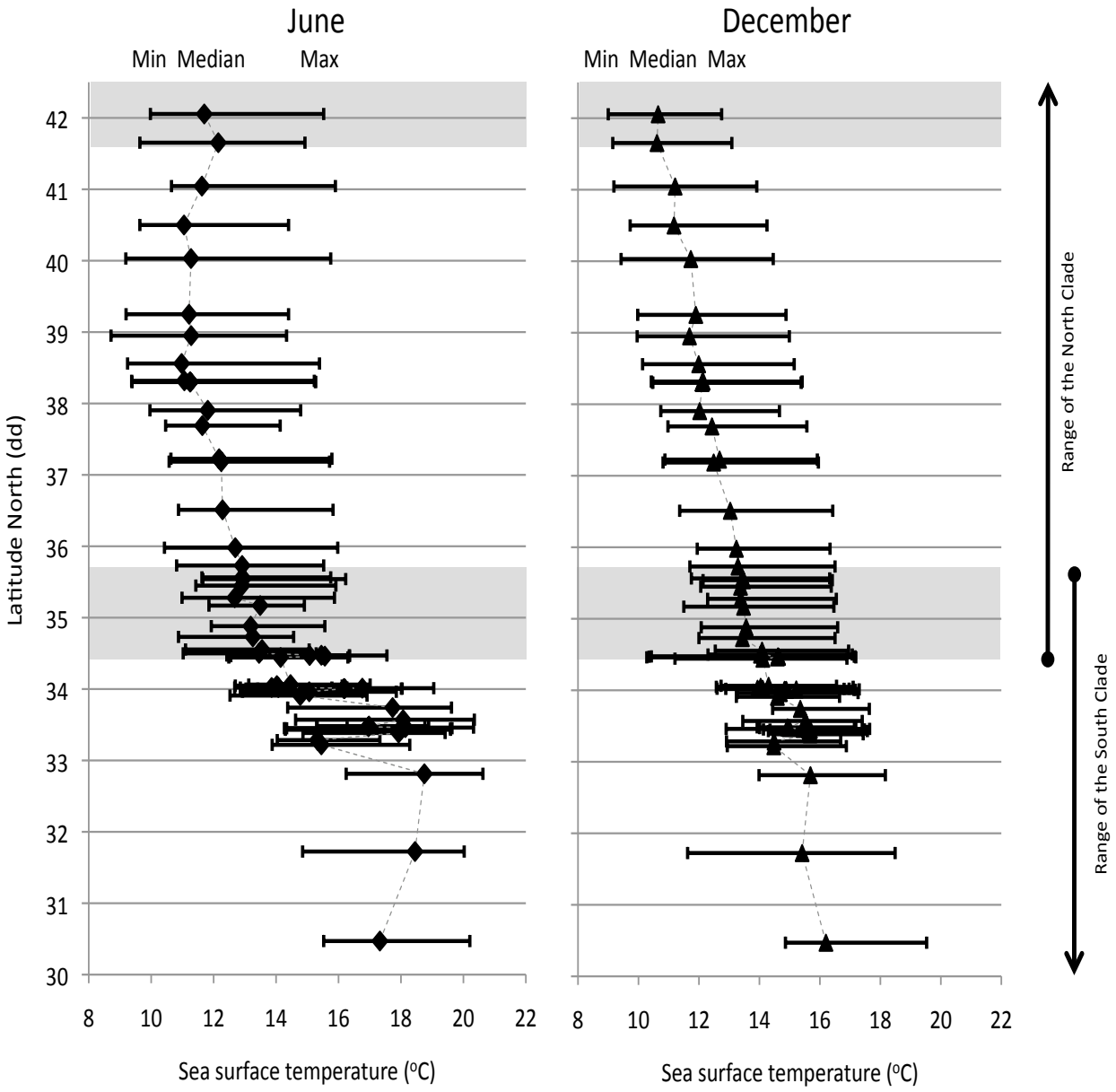

Figure 2.15: Latitudinal variation for monthly composites of sea chlorophyll-*a* in sea water for *Lottia scabra* sites for June and December from 1997 to 2006 from NOAA Coastwatch (http://coastwatch.pfeg.noaa.gov/erddap/griddap/erdSAchlamday.html). Concentration of chlorophyll-*a* in sea water range for June was 0.236 to 9.821 mg m^{-3}, with a median of 1.904 mg m^{-3}, and December was 0.247 to 4.795 mg m^{-3}, with a median of 1.142 mg m^{-3}. Error bars represent minimum and maximum temperatures. Shaded areas represent the nlNC, which is from 03-USCADCD (41.65°N) and extends north to 01-USORCAS (43.31°N, ~100 km north of graph, not shown), and the slNC from 22-USCAPSN (35.73°N) to 38-USCAArH (34.47°N).

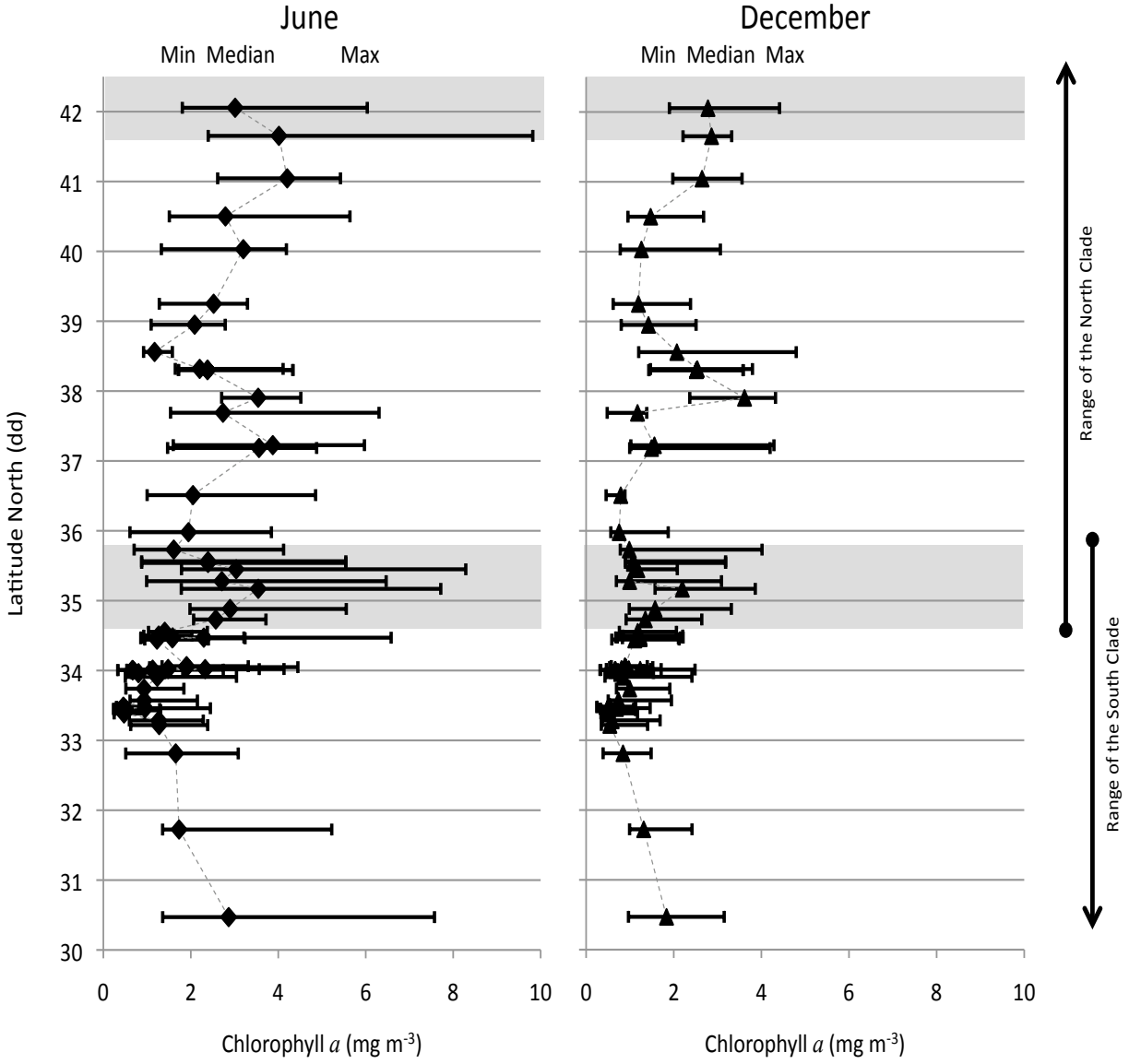

DISCUSSION:

In Table 1.1, the predicted characteristics of the hypotheses for the border populations range from small to large population size, low to high gene flow and/or genetic diversity, and few to prevalent unique alleles. The characteristics of environment range from gradual change at the margins to a dispersal route that is blocked or broken. I will use the phylogeography of *Lottia scabra* and the predicted characteristics of the hypothesized range limits to infer the causes and mechanisms in three different range limits of this low to medium dispersal species.

Evolutionary history from phylogeography

Point Conception on the coast of California has long been considered a break between the 'Oregonian' and 'Californian' provinces, although the phylogenies of many species do not correspond to the biogeography of the area (Palumbi, 1995; Burton, 1998). The Oregonian province is bathed in the cold water of the California Current with strong and persistent cold water upwelling (Parrish et al., 1981). The Californian province is markedly different in terms of SST, salinity, hydrography, dissolved oxygen, and topography (Briggs, 1974; Seapy and Littler, 1980; Browne, 1994), and the Southern California Bight is characterized by minimal offshore Ekman transport and a closed gyral circulation near the coast (Parrish et al., 1981).

The abundant center hypothesis (ACH), which predicts that species should have abundances greatest near the centre of their range, where environmental conditions are moderate and organisms best adapted, declining gradually with changing conditions toward the range boundaries, the point at which the environment becomes so extreme that populations cannot be sustained (Brown, 1984), has been widely used in theory describing range limits (Haldane, 1956; Mayr, 1963; Kirkpatrick and Barton, 1997; Bridle and Vines, 2006). However tests of this

hypothesis in the Northeastern Pacific rocky intertidal have not show an abundant center (Sagarin and Gaines, 2002; Gilman, 2005). Yet the ACH assumes gene flow connects all relevant populations, and so one might ask whether it is pertinent to species within which there are strong phylogeographic discontinuities. In California coastal marine taxa, low-dispersal taxa have high phylogeographic structure and 55% have cryptic north-south phylogeographic lineages (Dawson, 2001), which if these lineages were analyzed separately could produce different abundant centre results.

The haplotype networks, genetic diversity, and gene flow for the two markers 16S and COI of the previously cryptic NC and SC demonstrate a clear phylogeographic break in the region of Point Conception where these two Clades overlap, and the NC exhibits a phylogeography and a slightly skewed abundance centre distribution that corresponds to the biogeographic break of the region. Previously, abundances of *L. scabra* were interpreted as showing no evidence of an abundant centre distribution (Gilman, 2005), but total distribution of *L. scabra,* as opposed to clades, was included in that data analysis. Abundance in the NC is in accordance with the ACH, which showed small populations at the margins. In the NC and the SC, the phylogeography shows low genetic diversity, and Slatkin's linearized F_{ST} analysis showed isolation by distance resulting from high gene flow.

Inferring process from environmental pattern

Research in marine system dynamics that can affect distribution and range limits has provided evidence that marine systems are strongly driven by variation in change that vary with different environmental conditions including ocean temperature (Sanford, 1999), phytoplankton concentration and productivity, and water temperature during upwelling (Menge et al, 1997), and

precipitation in combination with factors such temperature, salinity, and tidal height (Dennis and Hellberg, 2010). In the region of the North Pacific dominated by the California Current, the most important environmental variables in the mid-zone (elevation tidal level) in rank were tide range, upwelling, air temperature, water temperature, precipitation, salinity, and wave period, and in the high zone, the key predictors in rank order were upwelling, precipitation, water and air temperature, tide range, and salinity (Schoch et al., 2006).

Intertidal animals are mostly of marine descent, but are subjected to aerial exposure at low tide that can lead to thermal stress and possible mortality from desiccation (Menge, 1978). Maximal air temperature can be a useful predictor of maximal body temperature in *Lottia gigantea*, but air temperature of the magnitude to be lethal is rare on the central California coast and only a fraction of the potentially lethal air temperatures overlap with low tides and calm seas (Denny et al., 2006). Cumulative physiological effects of acute sublethal temperatures, which can eventually lead to death or can have important implications for growth and reproduction, can possibly set the upper limit on temperature, and these effects may depend heavily on behavior or ecological interactions (Denny et al., 2006). For *L. scabra,* warmer air temperatures have a stronger effect than water temperature, particularly under limiting food conditions, and were associated with both higher mortality and lower maturation north of 36^{o}N (Gilman (2006b).

The effects of air temperature alone are not as important as when in combination with other dynamics. With exceptionally high air temperature, calm seas, and low tides, daily maximal solar irradiance also predicts maximal body temperature, but with less accuracy than daily maximal air temperature, and days when body temperature reached lethal levels (Denny et al., 2006). *Lottia gigantea* were able to survive much higher temperatures when kept in saturated air, and lethal temperatures were approximately 5°C lower in 50–60% relative

humidity conditions compared to 100% relative humidity trials (Miller et al., 2009). Relative humidity does not take into account the effect of temperature as do calculations for vapor pressure deficit (VPD), which is a metric of humidity that depends on temperature and is the difference of the amount of moisture in the air and how much moisture the air can hold when it is saturated.

Precipitation can play a role in humidity and high precipitation rates may affect local salinity and subsequently subtidal community structure by altering the spatial distributions of key predators (Witman and Grange, 1998). Oceanic salinity can be affected by multiple factors such as large river systems, but the high salinity and warm water of Southern California results from low input of fresh water and high rates of evaporation (Schoch et al., 2006). The higher salinity variation and cold water in Northern and Central California can be explained by the upwelling of bottom water along the portion of the coast most strongly influenced by the temporally consistent offshore advection of surface water (Schoch et al., 2006).

Upwelling, driven by winds, supplies nutrients to the coastal zones, which fuel the growth of phytoplankton, which is the base of productive coastal marine systems (Pauly and Christensen, 1995), and upwelling is a major mechanism for surface nutrient replacement (Parrish et al., 1981), which may strongly affect the structure and dynamics of nearshore communities (Menge et al., 1997). Along with the supply of nutrients, upwelling and relaxation dynamics have been found to have a strong connection to barnacle recruitment in central California (Roughgarden et al., 1991), and nutrients, microalgal productivity, and invertebrate grazer abundance were positively correlated (Menge et al., 1997). Chlorophyll-*a*, a proxy for nutrients (Halfar et al., 2004), can be correlated with upwelling, and persistent upwelling centers have been found to loosely coincide with notable regional peaks of chlorophyll-*a* off the

California coast (Broitman and Kinlan, 2006). Chlorophyll-*a* concentrations from SeaWiFS satellite data were in good agreement with *in situ* data (Broitman and Kinlan, 2006) and highly correlated (Halfar et al., 2004). In Monterey Bay California, low-chlorophyll waters corresponded with intrusion of offshore, low-salinity waters (Ryan et al., 2010).

The various environmental conditions at the three range limits showed a variety of results from very little change in precipitation in June in the slNC, to abrupt change in June in SST in the slNC. The predicted characteristics of the hypothesized causes of range limits in Table 1.1 in environmental change, along with genetic diversity, gene flow, population size, and unique alleles, can be used to infer the causes of range limits for *L. scabra.*

Causes of range limits from predicted characteristics

What causes the northern range limit of the North Clade?

In general, the degree of genetic diversity was higher in the nlNC and variation decreased compared to the range of the NC, and both the nlNC and the NC showed somewhat low genetic diversity overall. Low genetic diversity was predicted by the hypotheses genetically impoverished isolated population ($H_{1)}$, and 'leaky barrier' to dispersal with frequent immigration ($H_{4)}$. The higher diversity at the nlNC infers less frequent dispersal at the margin compared to the range of the NC, but that the population was not sustained by self-recruitment, so is it unlikely that the cause of the range limit is H_1. The hypothesis migration load (H_2) predicts high gene flow and genetic diversity, and H_4 predicts low gene flow and genetic diversity, and both causes predict small population size and few unique alleles.

Variation of environmental patterns is higher for all conditions in the range of the NC, compared to the nlNC for both June and December. While precipitation was higher at the nlNC

in June, little is know about salinity in this nearshore region because of lack of data, so there is little evidence that this increase in precipitation might be important for concentration of water salinity. The higher chlorophyll-*a* intensity and lower variation at the nlNC infers much higher upwelling, perhaps accompanied by less relaxation, which could influence recruitment. Relaxation is usually accompanied by elevated SST (Dahlhoff, 2004), and in the nlNC the minimum SST is higher compared to the range of the NC. Again in December, there was more precipitation at the nlNC, and more chlorophyll-*a* indicating higher upwelling, but both air temperature and SST intensity and variation were lower than the range of the NC inferring lower metabolism as warmer temperatures should raise metabolic rates and increase the demand for food (Dahlhoff et al., 2001; Sanford, 2002), and survival and maturation are greater for colder water temperature in the NC of *L. scabra* (Gilman, 2006b), so it seems likely that food shortage is not the reason for lower abundance found in the nlNC.

The nlNC showed a gradual change in environmental characteristics at the margin, which is predicted by H_1, H_2 and secular migration (H_{SM}). It is likely that the higher genetic diversity compared to the range of NC, even though low overall, and the gradual change of environmental change at the margin, with small population size, high gene flow, and few unique alleles infers that migration load is the most likely cause of the range limit for the nlNC.

What causes the southern range limit of the North Clade?

In general, genetic diversity was about the same or slightly decreased in the slNC, and variation greatly decreased in the slNC, except for nucleotide diversity in COI, with some differences in the two markers that could suggest a difference in selection, and the slNC showed somewhat low genetic diversity at the margin. Again as in the nlNC, low genetic diversity was predicted by H_1 and H_4, except genetic diversity decreased instead of increased at the margin. As in nlNC, H_2

predicts high gene flow and genetic diversity, and H_4 predicts low gene flow and genetic diversity, and both causes predict small population size and few unique alleles. The decreased genetic diversity at the margin might infer that the cause of 'leaky barrier' might be more important in the slNC than migration load, which has the predicted characteristic of high genetic diversity.

For environmental conditions, the most notable changes from the range of the NC to the slNC were a decrease in variation in June and December for all conditions. The decrease in chlorophyll-*a* concentration in sea-water intensity and variation, and the variation in salinity, in the slNC infers less upwelling resulting in a lower nutrient supply to the microalgae on the substrate, which could result in lower abundance in the slNC. Decreased upwelling could also influence successful recruitment and settlement of *L. scabra* compared to other organisms, because upwelling has been found to structure benthic communities by selective advection of propagules of some organisms, but not others (Schoch et al., 2006).

Survival, growth, and maturation are positively associated with chlorophyll-*a* concentrations on the substrate in the NC (Gilman, 2006b), and less upwelling resulting in a decrease of available nutrients, in combination with likely higher metabolism of *L. scabra* in warmer water, would result in the lower abundance in the slNC. SST increased slightly in the slNC in June (June SST was highly correlated with July-September SST), and average monthly SST continued to increase through September. Although this effect could result in lower abundance seen in the slNC, water temperature did not affect survival rates in the NC at higher latitudes (42^{o}N to 39^{o}N) where SST is much colder (Gilman, 2006b). Lower June humidity and higher air temperature in the slNC could affect survival, as survival is generally highest at cold air temperatures in the NC (Gilman, 2006b), and June air temperatures continue to rise through

September (June air temperature was highly correlated with July and August) extending the effect. Another possibility of the southern range limit of the North Clade could be a combination of factors and conditions that result in a different and detrimental community structure, such as an increase in predation or competition at the slNC.

The environmental characteristics at the margin showed an abrupt change or a dispersal route that is somewhat blocked by the pronounced change in SST and chlorophyll-*a,* which is predicted by H_4 and H_{SM}. The decreased genetic diversity at the margin might infer that the cause of H_4 might be more important in the slNC than H_2, which has the predicted characteristic of high genetic diversity. Incorporating these predicted characteristics with small population size and few unique alleles showed that the hypothesis with the most support for the range limit of the slNC is 'leaky barrier' with possible influence of migration load.

What causes the northern range limit of South Clade?

In general, diversity did not change between the ranges, but range of the SC variation was significantly higher compared to the nlSC, and the nlSC showed low to medium genetic diversity at the margin. These results again are predicted by H_1, and H_4. At the nlSC, since there is little change in genetic diversity compared to the range of the SC, it is not likely that genetics plays a large role in the causes of range limits, but does not rule out that genetic diversity has some effect. The lower variation at the margin could infer that there is some selection on the populations in this region, and the decreased abundance with high gene flow and few unique alleles infers that H_2 could be in combination with H_4, but overall genetic diversity showed that H_4 could be the most likely cause of range limit in the nlSC because selection might be at work at the barrier.

For environmental conditions, the most notable changes were in summer, where the nlSC showed a pronounced decrease in SST compared to the range of the SC, and SST intensity and variation greatly increased south of the slNC becoming much warmer and somewhat less varied in the most southern part of the range of the SC. While SST greatly increased to the south, chlorophyll-*a* decreased significantly in summer, with the same pattern in winter but less intense, which indicates a great disparity in conditions possibly relating to food supply and metabolism of *L. scabra* that might affect survival, and/or recruitment. The pronounced change in SST and chlorophyll-*a* at the margin showed an abrupt change in environment or a dispersal route that is mostly blocked, which is predicted by H_4 and H_{SM}. The predicted characteristics of a mostly blocked dispersal route, small population size, low genetic diversity, and few unique alleles showed that the hypothesis with the most support for the range limit of nlSC is 'leaky barrier' with possible influence of migration load.

CONCLUSION:

It is clear that the biogeographic break at Point Conception corresponds to the phylogeographic break of the NC and SC. Patterns of abundance and gene flow are similar at the nlNC and slNC where some environmental conditions show clear and distinctive latitudinal dissimilar patterns at slNC, but less so at nlNC. Although the different degrees in latitudinal patterns of genetic diversity are not great, there is an increase in diversity corresponding to environmental change towards and south of the boundary of the slNC where environmental change is the greatest. While some genetic and environmental patterns are ambiguous, there are some clear distinctions between the range limits, and although the interpretation of the results is complicated, the

predicted characteristics for genetic diversity and environmental conditions yield a somewhat consistent pattern (Table 4.1).

Table 4.1: Hypothesized conclusion of populations at the borders of ranges of *Lottia scabra* under four hypothesized causes of range limits and secular migration. Blue is the nlNC (43.3°C to 41.7°N). Purple is the slNC (35.7°N to 34.5°N). Red is the nlSC (35.7°N to 29.95°N).

A	H_1: Genetically impoverished isolated population	H_2: Migration load	H_3: Physical barrier to dispersal	H_4: Leaky barrier to dispersal with frequent immigration	B	H_{SM}: Secular migration (moderate gene flow)
Characteristics of environment (biotic or abiotic)					***Characteristics of environment***	
i. Environmental change at margin	Gradual change	Gradual change	Dispersal route blocked/broken	Dispersal route mostly blocked	i. Environmental change at margin	Gradual, stepped, or abrupt change
Size of marginal population					***Size of marginal population***	
ii. Marginal population size	Small	Declining toward border	Large	Large changing to small	ii. Marginal population size	Moderate – large
Border populations					***Border populations***	
iii. Gene flow	Low	High	Low/medium/high	Low	iii. Gene flow	Medium
iv. Genetic diversity	Low, decreasing toward margin	High	Medium/high	Low	iv. Genetic diversity	Moderate
v. Unique alleles	Prevalent	Few	Few/some	Few/some	v. Unique alleles	Some

For the nlNC, the mechanism with the greatest support is migration load (H_2), where high gene flow causes maladapted alleles to swamp alleles that may be locally adapted, and recruitment limitation a likely cause for lower abundance at the northern limit (Gilman, 2006a). For the slNC, and the boundary of the North and South Clades, two hypotheses are plausible,

migration load (H_2) and a "leaky" dispersal barrier (H_4), where dispersal is mostly blocked by either biotic or abiotic environmental characteristics, or a combination of both.

The analysis highlights the difficulty in establishing clear causes for range limits in non-model organisms, with each hypothesized cause gaining some support, but the hypothetical characteristics presented here can indentify probable mechanisms and causes of range limits in *L. scabra* and point to useful fields of study to further the understanding of its range limits. Comparison of the high dispersal *T. rubescens* and the low-medium dispersal *L. scabra* show that dispersal alone cannot infer the causes of range limits. This study also emphasizes the importance of identifying cryptic lineages in the study of range limits, and how the interpretations of the mechanisms and causes of range limits can be misconstrued when genetic information is lacking. While there are difficulties in working with loci that may or may not be involved in setting range limits, it is still possible to establish differences between range limits that can point to areas of further consideration of how different measures and levels of genetic diversity may inform us about, and influence, the evolutionary dynamics of range limits. For *L. scabra*, much could be learned from experiments involving the NC and SC's performance in contrasting environmental conditions, especially upwelling, at the boundary of these two distinct Clades.

ACKNOWLEDGEMENTS:

Funding: University of California Marine Council's Coastal Environmental Quality Initiative; Mellon Foundation; D. Eernisse acknowledges a sabbatical fellowship supported by the National Evolutionary Synthesis Center (NESCent), NSF #EF-0423641. Thank you to Pete Raimondi and the PISCO SWAT team, H. Livingston, and R. Sagarin for abundance data. Kristen Kusic Heady, E. Sanford, S. Gilman, L. Crummett, J. Fernandez, G. Miller-Messner, S. Morgan, and D. Richards (Wrigley Institute) for collections. Staff at Bodega Marina lab, L. Laughrin (UC Santa Cruz Island reserve), D. Canestro (Kenneth S. Norris UC Marine Reserve), R. Burton, I. Kay, E. Kisfaludy, K. Roy (UC San Diego, Scripps Coastal Reserve), H. Helling (Ocean Institute, Dana Point Marine Life Refuge), K. Boutillier, L. Garske (Wrigley Marine Science Center), L. Valentine (Bodega Marine Lab) for assisting in local logistics that made collecting possible. Miguel Fernandez for distance data. R. Kelly assisted with preliminary analyses of 16S for *L. scabra* and outgroup taxa. Cynthia Hays, J. Vo, K. Bayha, M. Fernandez, H. Swift, L. Gómez-Daglio, L. Schiebelhut, and A. Nandipati for lab support. And special thanks to Michael N Dawson for conceiving this study, coordinating the design, feedback, and helping with preparations. Collections were made under CDFG permit 802024-03 and CA State Parks permit 51933.

REFERENCES:

Banks SC, Ling SD, Johnson CR, Piggott MP, Williamson JE, Beheregaray LB (2010) Genetic structure of a recent climate change-driven range extension. *Molecular Ecology.* 1**9,** 2011-2024.

Bickford D, Lohman DJ, Sodhi NS, Ng PKL, Meier R, Winker K, Ingram KK, Das I (2007) Cryptic species as a window on diversity and conservation. *Trends in Ecology and Evolution.* **22,** 148-155.

Bridle JR, Vines TH (2006) Limits to evolution at range margins: when and why does adaptation fail? *Trends in Ecology and Evolution*. **22,** 140-147.

Briggs JC (1974) *Marine Zoogeography*. McGraw-Hill, NewYork.

Broitman BR, Kinlan BP (2006) Spatial scales of benthic and pelagic producer biomass in a coastal upwelling ecosystem. *Marine Ecology Progress Series.* **15,** 15-25

Brown JH (1984) On the relationship between abundance and distribution of species. *American Naturalist.* **124,** 255-279.

Browne, D.R. (1994) Understanding the oceanic circulation in and around the Santa Barbara Channel. *The Fourth California Islands Symposium: Update on the Status of Resources* (eds. by WL Halvorson and GJ Maender), pp. 27-34. Santa Barbara Museum of Natural History, Santa Barbara.

Burton, R.S. (1998) Intraspecific phylogeography across the Point Conception biogeographic boundary. *Evolution.* **52,** 734-745.

Clement M, Posada D, Crandell KA (2000) TCS: a computer program to estimate gene genealogies. *Molecular Ecology.* **9,** 1657-1659.

Cunningham CW, Buss LW (1993) Molecular Evidence for Multiple Episodes of Paedomorphosis in the Family Hydractiniidae. *Biochemical Systematics and Ecology.* **21,** 57-69.

Dahlhoff EP, Buckley BA, Menge BA (2001) Physiology of the rocky intertidal predator *Nucella ostrina* along an environmental stress gradient. *Ecology.* **82,** 2816-2829

Dahlhoff EP (2004) Biochemical indicators of stress and metabolism: Applications for Marine Ecological Studies. *Annual Review of Physiology*. **66,** 183-207

Dawson MN, Raskoff KA, Jacobs DK (1998) Preservation of marine invertebrate tissues for DNA analyses. *Molecular Marine Biology and Biotechnology*. **7**, 145-152

Dawson MN (2001) Phyloegeography in coastal marine animals: a solution in California? *Journal of Biogeography.* **28,** 723-736.

Dawson MN (2004) Some implications of molecular phylogenetics for understanding biodiversity in jellyfishes, with emphasis on Scyphozoa. *Hydrobiologia.* **530/531,** 249-260.

Dawson MN, Grosberg RK, Stuart YE, Sanford E (2010) Population genetic analysis of a recent range expansion: mechanisms regulating the poleward range limit in the volcano barnacle *Tetraclita rubescens*. *Molecular Ecology*. **19,** 1585-1605.

Dennis AB, Hellberg ME (2010) Ecological partitioning among parapatric cryptic species. *Molecular Ecology.* **19,** 3206–3225.

Denny MW, Miller LP, Harley CDG (2006) Thermal stress on intertidal limpets: long-term hindcasts and lethal limits. *The Journal of Experimental Biology.* **209,** 2420-2431.

Doak DF, Morris WF (2010) Demographic compensation and tipping points in climate-induced range shifts. *Nature.* **467,** 959-962.

Eckert CG, Samis KE, Lougheed SC (2008) Genetic variation across species' geographical ranges: the central–marginal hypothesis and beyond. *Molecular Ecology*. **17,** 1170-1188.

Ellstrand NC, Elam DR (1993) Population genetic consequences of small population size: implications for plant conservation. *Annual Review of Ecology and Systematics.* **24,** 217-242.

Excoffier L, Lischer HEL (2010) Arlequin suite ver 3.5: A new series of programs to perform population genetics analyses under Linux and Windows. *Molecular Ecology Resources.* **10,** 564-567.

Folmer O, Black M, Hoeh W, Lutz R, Vrijenhoek R (1994) DNA primers for amplification of mitochondrial cytochrome *c* oxidase subunit I from diverse metazoan invertebrates. *Molecular Marine Biology and Biotechnology*. **3,** 294-299.

Gaston KJ (2003) *The Structure and Dynamics of Geographic Ranges*. Oxford University Press, New York.

Gaylord B, Gaines SD (2000) Temperature or transport? Range limits in marine species mediated solely by flow. *American Naturalist.* **155,** 769-789.

Gilman S (2005) A test of Brown's principle in the intertidal limpet *Collisella scabra* (Gould, 1846). *Journal of Biogeography.* **32,** 1583-1589.

Gilman SE (2006a) The northern geographic range limit of the intertidal limpet *Collisella scabra*: a test of performance, recruitment, and temperature hypotheses. *Ecography.* **26,** 1-12.

Gilman SE (2006b) Life at the edge: an experimental study of a poleward range boundary. *Oecologia.* **148,** 270-279.

Gomulkiewicz R, Holt RD, Barfield M (1999) The effects of density dependence and immigration on local adaptation and niche evolution in a black-hole sink environment. *Theoretical Population Biology.* **55,** 283-296.

Haldane JBS (1956) The relation between density regulation and natural selection. *Proceedings of the Royal Society of London, Series B*. **145,** 306–308.

Halfar J, Godinez-Orta L, Mutti M, Valdez-Holguin JE, Borges JM. (2004) Nutrient and temperature controls on modern carbonate production: An example from the Gulf of California, Mexico. *Geology*. **32,** 213-216.

Helmuth B, Kingsolver JG, Carrington E (2005) Biophysics, physiological ecology, and climate change: does mechanism matter? *Annual Review of Physiology*. **67,** 177-201.

Hoffmann AA, Blows MW (1993) Evolutionary genetics an climate change—will animals adapt to global warming. In: *Biotic Interactions and Global Change* (eds. PM Kareiva, JG Kingsolver, RB Huey), pp. 165–178. Sinauer, Sunderland, MA.

Hoffmann AA, Blows MW (1994) Species borders: ecological and evolutionary perspectives. *Trends in Ecology and Evolution.* **9,** 223-227.

Holt RD (2003) On the evolutionary ecology of species' ranges. *Evolutionary Ecology Research.* **5,** 159-178.

Holt, RD (2009) Bringing the Hutchinsonian niche into the 21st century: Ecological and evolutionary perspectives. *Proceedings National Academy of Sciences USA* **106**, 19659-19665.

Hutchins LW (1947) The basis for temperature zonation in geographical distribution. *Ecological Monographs.* **17,** 325-335.

Jeanmougin F, Thompson JD, Gouy M, Higgins DG, Gibson TJ (1998) Multiple sequence alignment with Clustal X. *Trends in Biochemical Sciences.* **23**, 403-405.

Joly S, Stevens MI, van Vuuren BJ (2007) Haplotype networks can be misleading in the presence of missing data. *Systematic Biology.* **56,** 857-862.

Jones SJ, Mieszkowska N, Wethey DS (2009) Linking thermal tolerances and biogeography: *Mytilus edulis* (L.) at its southern limit on the East Coast of the United States. *Biological Bulletin*. **217,** 73-85.
Kirkpatrick M, Barton NH (1997) Evolution of a species' range. *American Naturalist*. **150,** 1-23.
Kuo ESL, Sanford E (2009) Geographic variation in the upper thermal limits of an intertidal snail: implications for climate envelope models. *Marine Ecology Progress Series.* **388,** 137-146.
Lomolino MV, Riddle BR, Brown JH (2005) Biogeography, 3rd ed. Sinauer, Sunderland, MA.
Mayr E (1963) *Animal Species and Evolution*. Oxford University Press, London.
Menge BA (1978) Predation intensity in a rocky intertidal community. Relation between predator foraging activity and environmental harshness. *Oecologia.* **34,** 1-16.
Menge BA, Daley BA, Wheeler PA, Dahlhoff E, Sanford E, Strub PT (1997) Benthic-pelagic links and rocky intertidal communities: Bottom-up effects on top-down control? *Proceedings National Academy of Sciences USA.* **94,** 14530–14535.
Miller LP, Harley CDG, Denny MW (2009) The role of temperature and desiccation stress in limiting the local-scale distribution of the owl limpet, *Lottia gigantea. Functional Ecology.* **23,** 756–767.
Morris RH, Abbott DP, Haderlie EC (1980) *Intertidal invertebrates of California*. Stanford University Press, Stanford California.
Palumbi, S.R. (1995) Using genetics as an indirect estimator of larval dispersal. *Ecology of Marine Invertebrate Larvae* (ed. by LR McEdward), pp. 396-387. CRC Press, Boca Raton.
Palumbi SR (1996) Nucleic acids II: The polymerase chain reaction. In (eds. DM Hillis, C Moritz, MK Mable (eds), *Molecular Systematics,* 2nd ed. Sinauer Assoc., Inc., Sunderland, MA, pp. 205-247.
Parmesan C, Yohe G (2003) A globally coherent fingerprint of climate change impacts across natural systems. *Nature.* **421,** 37-42.
Parrish RH, Nelson CS, Bakun A (1981) Transport mechanisms and reproductive success in fishes of the California Current. *Biological Oceanography.* **1,** 175-203.
Pauly D, Christensen V (1995) Primary production required to sustain global fisheries. *Nature.* **374,** 255-257.
Perry AL, Low PJ, Ellis JR, Reynolds JD (2005) Climate change and distribution shifts in marine fishes. *Science*. **308,** 1912-1915.
Pfenninger M, Schwenk K (2007) Cryptic animal species are homogeneously distributed among taxa and biogeographical regions. *BMC Evolutionary Biology.* **7,** 121.
Pitt NR, Poloczanska ES, Hobday AJ (2010) Climate-driven range changes in Tasmanian intertidal fauna. *Marine and Freshwater Research***. 61,** 963-970.
Roughgarden J, Pennington JT, Stoner D, Alexander S, Miller K (1991) Collisions of upwelling fronts with the intertidal zone: The cause of recruitment pulses in barnacle populations of central California. *Acta Oecologica.* **12,** 35–51.
Ryan JP, McManus MA, Sullivan JM (2010) Interacting physical, chemical and biological forcing of phytoplankton thin-layer in Monterey Bay, California. *Continental Shelf Research*. **30,** 7-16.
Sagarin RD, Barry JP, Gilman SE, Baxter CH (1999) Climate-related change in an intertidal community over short and long time scales. *Ecological Monographs.* **69,** 465-490.
Sagarin RD and Gaines SD (2002) Geographical abundance distributions of coastal invertebrates: using one-dimensional ranges to test biogeographic hypotheses. *Journal of*

Biogeography. **29**, 985-997.
Sanford E (1999) Regulation of keystone predation by small changes in ocean temperature. *Science.* **283**, 2095-2097.
Sanford E (2002) Water temperature, predation, and the neglected role of physiological rate effects in rocky intertidal communities. *Integrative and Comparative Biology.* **42,** 881-891.
Schoch GC, Menge BA, Allison G, Kavanaugh M, Thompson SA, Wood SA (2006) Fifteen degrees of separation: Latitudinal gradients of rocky intertidal biota along the California Current. *Limnology and Oceanography*. **51**, 2564-2585.
Seapy RR, Littler MM (1980) Biogeography of rocky intertidal macroinvertebrates. *The California Islands: Proceedings of a Multi-Disciplinary Symposium* (ed. by DM Powers), pp. 307-323. Santa Barbara Museum of Natural History, Santa Barbara.
Sexton JP, McIntyre PJ, Angert AL, Rice KJ (2009) Evolution and Ecology of Species Range Limits. *Annual Review of Ecology, Evolution, and Systematics.* **40,** 415–436.
Simison WB, Lindberg DR, Boore JL (2006) Rolling circle amplification of metazoan mitochondrial genomes. *Molecular Phylogenetics and Evolution*, **39,** 562-567
Strathmann MF (1987) *Reproduction and development of marine invertebrates of the northern Pacific coast: data and methods for the study of eggs, embryos, and larvae*. University of Washington Press, Seattle, Wash.
Sutherland JP (1970) Dynamics of high and low populations of the limpet *Acmaea scabra* (Gould). *Ecology Monographs.* **40,** 169-188.
Swofford DL (2002) PAUP*: phylogenetic analysis using parsimony (*and other methods) Version 4. Sinauer Associates, Sunderland.
U.S. National Oceanographic Data Center: Global Temperature–Salinity Profile Program. June 2006. *U.S. Department of Commerce, National Oceanic and Atmospheric Administration*, National Oceanographic Data Center, Silver Spring, Maryland, 20910. (http://www.nodc.noaa.gov/GTSPP/).
Witman J D, Grange KR (1998) Links between rain, salinity, and predation in a rocky subtidal community. *Ecology* **79,** 2429–2447.

APPENDIX:

Table S1: Site numbers, locations, acronyms, GPS coordinates, and sample sizes for *Lottia scabra*.

Site #	Location, county/region, state, country	Site acronym	°N (dd)	°W (dd)	*n*
01	Cape Arago, Coos, OR, USA	USORCAS	43.310	-124.400	5
02	Brookings, Curry, OR, USA	USORBro	42.055	-124.250	12
03	Damnation Creek, Del Norte, CA, USA	USCADCD	41.653	-124.130	10
04	Trinidad, Humboldt, CA, USA	USCATrn	41.045	-124.130	10
05	Cape Mendocino, Humboldt, CA, USA	USCACpM	40.500	-124.300	13
06	Shelter Cove, Humboldt, CA, USA	USCASCH	40.031	-124.079	27
07	Fort Bragg, Mendocino, CA, USA	USCAFBM	39.250	-123.805	13
08	Point Arena, Mendocino, CA, USA	USCAPAM	38.950	-123.730	21
09	Salt Point, Sonoma, CA, USA	USCASAL	38.560	-123.325	19
10	Bodega Reserve, Sonoma, CA, USA	USCABRS	38.318	-123.073	15
11	Bodega Head, Sonoma, CA, USA	USCABHS	38.303	-123.053	16
12	Bodega Jetty, Sonoma, CA, USA	USCABJS	38.300	-123.050	15
13	Bolinas Point, Marin, CA, USA	USCABPM	37.904	-122.727	15
14	Pillar Point, San Mateo, CA, USA	USCAPPS	37.500	-122.500	6
15	Southeast, Farallon Islands, CA, USA	USCAFAR	37.690	-123.003	8
16	Bean Creek, San Mateo, CA, USA	USCABeC	37.226	-122.411	10
17	Pigeon Point, San Mateo, CA, USA	USCAPiP	37.185	-122.397	15
18	Scott Creek, Santa Cruz, CA, USA	USCAScC	37.045	-122.237	6
19	Stillwater Cove, Monterey, CA, USA	USCASwC	36.561	-121.940	5
20	Point Lobos, Monterey, CA, USA	USCAPLM	36.511	-121.941	15
21	Mill Creek, Monterey, CA, USA	USCAMiC	35.980	-121.491	9
22	Point Sierra Nevada, San Luis Obispo, CA, USA	USCAPSN	35.731	-121.324	16
23	Cambria, San Luis Obispo, CA, USA	USCACam	35.564	-121.090	15
24	Rancho Marino, San Luis Obispo, CA, USA	USCARaM	35.540	-121.090	10
25	Cayucos, San Luis Obispo, CA, USA	USCACay	35.449	-120.940	15
26	Hazards, San Luis Obispo, CA, USA	USCAHaz	35.279	-120.888	14
27	Shell Beach, San Luis Obispo, CA, USA	USCAShB	35.169	-120.696	23
28	Occulto, Santa Barbara, CA, USA	USCAOcc	34.881	-120.639	23
29	Purisima, Santa Barbara, CA, USA	USCAPur	34.755	-120.641	6
30	Stairs, Santa Barbara, CA, USA	USCASTR	34.731	-120.615	20
31	Boathouse, Santa Barbara, CA, USA	USCABoH	34.554	-120.611	24
32	Jalama Co. Park, Santa Barbara, CA, USA	USCAJAL	34.500	-120.500	11
33	Government Point, Santa Barbara, CA, USA	USCAGoP	34.442	-120.456	8
34	San Augistin Beach 2, Santa Barbara, CA, USA	USCASAu	34.450	-120.380	6
35	San Augistin Beach 1, Santa Barbara, CA, USA	USCASAB	34.450	-120.380	5
36	Alegria, Santa Barbara, CA, USA	USCAAle	34.470	-120.270	7
37	Gaviota State Park, Santa Barbara, CA, USA	USCAGSP	34.470	-120.230	8
38	Arroyo Hondo, Santa Barbara, CA, USA	USCAArH	34.474	-120.144	14
39	Refugio State Beach, Santa Barbara, CA, USA	USCARSB	34.461	-120.073	12
40	Cuyler Harbor, San Miguel Is., CA, USA	USCACuH	34.048	-120.336	15
41	Crook Point, San Miguel Is., CA, USA	USCACrP	34.022	-120.379	15
42	Mussel Shoals, Ventura, CA, USA	USCAMuS	34.350	-119.440	5
43	Fraser Point, Santa Cruz Is., CA, USA	USCAFrP	34.063	-119.919	15
44	Prisoners Harbor, Santa Cruz Is., CA, USA	USCAPrH	34.020	-119.687	7
45	Willows, Santa Cruz Is., CA, USA	USCAWil	33.962	-119.755	15
46	Coches Prietos, Santa Cruz Is., CA, USA	USCACoP	33.970	-119.720	6
47	Leo Carillo State Beach, Los Angeles, CA, USA	USCALCB	34.050	-118.930	4
48	Paradise Cove, Los Angeles, CA, USA	USCAPaC	34.012	-118.793	15
49	Lobo Canyon, Santa Rosa Is., CA, USA	USCALoC	34.020	-120.100	15
50	Johnson's Lee, Santa Rosa Is., CA, USA	USCAJoL	33.909	-120.087	15
51	Frenchy's Cove, Anacapa Is., CA, USA	USCAFrC	34.007	-119.411	15
52	Middle Anacapa, Anacapa Is., CA, USA	USCAMAI	34.006	-119.396	15
53	Point Vicente, Los Angeles, CA, USA	USCAPtV	33.740	-118.410	10
54	Crystal Cove, Orange, California, USA	USCACCO	33.571	-117.838	12
55	Landing Cove, Santa Barbara Is., CA, USA	USCALaC	33.482	-119.029	15
56	Sea Lion Rookery, Santa Barbara Is., CA, USA	USCASLR	33.472	-119.031	15
57	South Laguna Beaches, Orange, CA, USA	USCASLB	33.500	-117.750	5
58	Dana Point, Orange, CA, USA	USCADaP	33.460	-117.714	8
59	Bird Rock, Santa Catalina Is., CA, USA	USCABiR	33.452	-118.488	15
60	Isthmus Cove, Santa Catalina Is., CA, USA	USCAIsC	33.450	-118.500	8
61	Pin Rock, Santa Catalina Is., CA, USA	USCAPiR	33.430	-118.500	9
62	Little Harbor, Santa Catalina Is., CA, USA	USCALiH	33.385	-118.475	14
63	Thousand Springs, San Nicholas Is., CA, USA	USCAThS	33.285	-119.530	15
64	Marker Poles, San Nicholas Is., CA, USA	USCAMaP	33.219	-119.496	15
65	Scripps Pier / La Jolla, San Diego, CA, USA	USCAScS	32.871	-117.253	6
66	Bird Rock / La Jolla, San Diego, CA, USA	USCABLJ	32.813	-117.274	14
67	La Bufadora, Baja California, Mexico	MXBCBuf	31.724	-116.714	13
68	El Puerto de Santo Tomas, Baja CA, Mexico	MXBCPST	31.550	-116.680	2
69	La Chorera, Baja California, Mexico	MXBCCho	30.470	-116.047	13
70	Punta Baja, Baja California, Mexico	MXBCPBj	29.949	-115.812	4

Table S2: Genetic diversity in mitochondrial markers 16S and COI for *Lottia scabra* for the North and South Clades.

		Northern Clan								*Southern Clan*							
Site #	Site acronym	16S n_s	16S n_a	16S $h \pm$ SD	16S $\pi \pm$ SD	COI n_s	COI n_a	COI $h \pm$ SD	COI $\pi \pm$ SD	16S n_s	16S n_a	16S $h \pm$ SD	16S $\pi \pm$ SD	COI n_s	COI n_a	COI $h \pm$ SD	COI $\pi \pm$ SD
02	USORBro	12	4	0.6970 ± 0.0904	0.0021 ± 0.0017	12	3	0.4394 ± 0.1581	0.0010 ± 0.0010								
03	USCADCD	10	2	0.2000 ± 0.1541	0.0004 ± 0.0006	10	1	0.0000 ± 0.0000	0.0000 ± 0.0000								
04	USCATrn	10	3	0.5111 ± 0.1643	0.0011 ± 0.0012	10	3	0.3778 ± 0.1813	0.0008 ± 0.0010								
05	USCACpM	13	3	0.2949 ± 0.1558	0.0006 ± 0.0008	13	2	0.1538 ± 0.1261	0.0003 ± 0.0005								
06	USCASCH	27	4	0.3846 ± 0.1081	0.0008 ± 0.0009	27	3	0.2108 ± 0.1005	0.0005 ± 0.0006								
07	USCAFBM	13	2	0.4615 ± 0.1096	0.0009 ± 0.0010	13	3	0.2949 ± 0.1558	0.0007 ± 0.0008								
08	USCAPAM	21	2	0.4286 ± 0.0891	0.0009 ± 0.0009	21	3	0.1857 ± 0.1102	0.0004 ± 0.0006								
09	USCASAL	19	4	0.4503 ± 0.1282	0.0010 ± 0.0010	19	4	0.2982 ± 0.1329	0.0009 ± 0.0010								
10	USCABRS	15	3	0.2571 ± 0.1416	0.0008 ± 0.0009	15	3	0.4476 ± 0.1345	0.0010 ± 0.0010								
11	USCABHS	16	4	0.5750 ± 0.1150	0.0014 ± 0.0013	16	2	0.1250 ± 0.1064	0.0003 ± 0.0005								
12	USCABJS	15	2	0.4762 ± 0.0920	0.0010 ± 0.0010	15	3	0.2571 ± 0.1416	0.0006 ± 0.0007								
13	USCABPM	15	3	0.5143 ± 0.1164	0.0012 ± 0.0011	15	2	0.1333 ± 0.1123	0.0003 ± 0.0005								
15	USCAFAR	8	4	0.7500 ± 0.1391	0.0019 ± 0.0017	8	3	0.4643 ± 0.2000	0.0011 ± 0.0011								
16	USCABeC	10	2	0.3556 ± 0.1591	0.0007 ± 0.0009	10	2	0.2000 ± 0.1541	0.0004 ± 0.0006								
17	USCAPiP	15	1	0.0000 ± 0.0000	0.0000 ± 0.0000	15	1	0.0000 ± 0.0000	0.0000 ± 0.0000								
20	USCAPLM	15	3	0.3619 ± 0.1448	0.0008 ± 0.0009	15	1	0.0000 ± 0.0000	0.0000 ± 0.0000								
21	USCAMiC	9	3	0.4167 ± 0.1907	0.0009 ± 0.0010	9	1	0.0000 ± 0.0000	0.0000 ± 0.0000								
22	USCAPSN	11	4	0.6000 ± 0.1539	0.0014 ± 0.0013	12	2	0.3030 ± 0.1475	0.0006 ± 0.0008	5	2	0.4000 ± 0.2373	0.0008 ± 0.0010	4	2	0.5000 ± 0.2652	0.0011 ± 0.0013
23	USCACam	14	3	0.3846 ± 0.1494	0.0008 ± 0.0009	14	2	0.1429 ± 0.1188	0.0003 ± 0.0005	1	1			1	1		
24	USCARaM	10	3	0.3778 ± 0.1813	0.0008 ± 0.0010	10	1	0.0000 ± 0.0000	0.0000 ± 0.0000	0				0			
25	USCACay	15	3	0.5333 ± 0.1259	0.0012 ± 0.0011	15	2	0.1333 ± 0.1123	0.0003 ± 0.0005	0				0			
26	USCAHaz	13	2	0.2821 ± 0.1417	0.0006 ± 0.0007	13	2	0.1538 ± 0.1261	0.0003 ± 0.0005	1	1			1	1		
27	USCAShB	21	4	0.5571 ± 0.0922	0.0012 ± 0.0011	21	1	0.0000 ± 0.0000	0.0000 ± 0.0000	2	1	0.0000 ± 0.0000	0.0000 ± 0.0000	2	2	1.0000 ± 0.5000	0.0021 ± 0.0030
28	USCAOcc	22	3	0.3247 ± 0.1173	0.0007 ± 0.0008	22	2	0.0909 ± 0.0809	0.0002 ± 0.0004	1	1			1	1		
30	USCASTR	17	3	0.4706 ± 0.1177	0.0010 ± 0.0010	17	5	0.4265 ± 0.1468	0.0010 ± 0.0010	3	2	0.6667 ± 0.3143	0.0013 ± 0.0017	3	2	0.6667 ± 0.3143	0.0014 ± 0.0018
31	USCABoH	17	2	0.2206 ± 0.1208	0.0004 ± 0.0006	17	3	0.2279 ± 0.1295	0.0005 ± 0.0007	7	4	0.7143 ± 0.1809	0.0023 ± 0.0019	7	3	0.5238 ± 0.2086	0.0028 ± 0.0023
32	USCAJAL	5	2	0.6000 ± 0.1753	0.0012 ± 0.0013	6	2	0.3333 ± 0.2152	0.0028 ± 0.0023	6	2	0.3333 ± 0.2152	0.0013 ± 0.0014	5	2	0.4000 ± 0.2373	0.0009 ± 0.0011
33	USCAGoP	2	1	0.0000 ± 0.0000	0.0000 ± 0.0000	2	2	1.0000 ± 0.5000	0.0021 ± 0.0030	6	1	0.0000 ± 0.0000	0.0000 ± 0.0000	6	2	0.3333 ± 0.2152	0.0007 ± 0.0009
37	USCAGSP	0				0				8	3	0.6071 ± 0.1640	0.0016 ± 0.0014	8	2	0.4286 ± 0.1687	0.0009 ± 0.0010
38	USCAArH	1	1			1	1			13	4	0.6026 ± 0.1306	0.0020 ± 0.0016	13	3	0.4103 ± 0.1539	0.0018 ± 0.0015
39	USCARSB									12	4	0.4545 ± 0.1701	0.0016 ± 0.0014	12	3	0.5303 ± 0.1359	0.0021 ± 0.0017
40	USCACuH									15	5	0.6286 ± 0.1253	0.0019 ± 0.0015	15	3	0.3619 ± 0.1448	0.0016 ± 0.0014
41	USCACrP									15	3	0.4476 ± 0.1345	0.0010 ± 0.0010	15	2	0.1333 ± 0.1123	0.0003 ± 0.0005
43	USCAFrP									15	2	0.1333 ± 0.1123	0.0005 ± 0.0007	15	4	0.6000 ± 0.1129	0.0021 ± 0.0017
45	USCAWil									15	4	0.5524 ± 0.1374	0.0017 ± 0.0015	15	3	0.3619 ± 0.1448	0.0023 ± 0.0018
48	USCAPaC									15	6	0.7619 ± 0.0813	0.0024 ± 0.0018	15	6	0.5714 ± 0.1489	0.0022 ± 0.0017
49	USCALoC									15	6	0.7048 ± 0.1139	0.0024 ± 0.0018	15	3	0.3619 ± 0.1448	0.0024 ± 0.0018
50	USCAJoL									15	7	0.6571 ± 0.1384	0.0019 ± 0.0015	15	2	0.1333 ± 0.1123	0.0011 ± 0.0011
51	USCAFrC									15	7	0.7238 ± 0.1206	0.0025 ± 0.0019	15	4	0.5524 ± 0.1374	0.0028 ± 0.0021
52	USCAMAI									15	4	0.6857 ± 0.1040	0.0022 ± 0.0017	15	3	0.3619 ± 0.1448	0.0024 ± 0.0018
53	USCAPtV	1	1							9	2	0.5000 ± 0.1283	0.0010 ± 0.0011	10	3	0.3778 ± 0.1813	0.0008 ± 0.0010
54	USCACCO									12	2	0.1667 ± 0.1343	0.0003 ± 0.0005	12	2	0.1667 ± 0.1343	0.0007 ± 0.0008
55	USCALaC									15	3	0.5143 ± 0.1164	0.0014 ± 0.0012	15	2	0.1333 ± 0.1123	0.0011 ± 0.0011
56	USCASLR									15	4	0.6286 ± 0.1235	0.0020 ± 0.0016	15	3	0.5333 ± 0.1259	0.0026 ± 0.0019
58	USCADaP									8	2	0.2500 ± 0.1802	0.0005 ± 0.0007	8	1	0.0000 ± 0.0000	0.0000 ± 0.0000
59	USCABiR									15	3	0.3619 ± 0.1448	0.0001 ± 0.0010	15	3	0.2571 ± 0.1416	0.0014 ± 0.0013
60	USCAIsC									8	3	0.4643 ± 0.2000	0.0010 ± 0.0011	8	1	0.0000 ± 0.0000	0.0000 ± 0.0000
61	USCAPiR									9	3	0.4167 ± 0.1907	0.0017 ± 0.0015	9	2	0.3889 ± 0.1644	0.0008 ± 0.0001
62	USCALiH									14	3	0.2747 ± 0.1484	0.0009 ± 0.0009	14	3	0.2747 ± 0.1484	0.0015 ± 0.0013
63	USCAThS									15	3	0.6762 ± 0.0696	0.0026 ± 0.0019	15	3	0.5619 ± 0.0954	0.0043 ± 0.0029
64	USCAMaP									15	3	0.3619 ± 0.1448	0.0013 ± 0.0012	15	3	0.3619 ± 0.1448	0.0023 ± 0.0018
66	USCABLJ									14	3	0.3846 ± 0.1494	0.0011 ± 0.0011	14	3	0.6044 ± 0.0759	0.0020 ± 0.0016
67	MXBCBuf									13	4	0.5256 ± 0.1527	0.0018 ± 0.0050	13	3	0.5897 ± 0.1219	0.0029 ± 0.0021
69	MXBCCho									13	3	0.5641 ± 0.1117	0.0022 ± 0.0017	13	4	0.7564 ± 0.0698	0.0041 ± 0.0028

Table S3: Environmental conditions with values for range areas.

	nINC 43.31°N to 41.65°N				**Range of the NC** 43.31°N to 34.47°N				**sINC** 35.73°N to 34.47°N				**Range of the SC** south of 35.73°N			
	minimum intensity	median intensity	maximum intensity	max-min variation	minimum intensity	median intensity	maximum intensity	max-min variation	minimum intensity	median intensity	maximum intensity	max-min variation	minimum intensity	median intensity	maximum intensity	max-min variation
June																
Air temp. (°C)	14.91	16.26	18.23	3.32	12.16	18.52	25.58	13.42	14.07	19.23	24.26	10.19	11.08	17.69	24.68	13.59
Precipitation (cm/day)	0	0.16	0.56	0.55	0	0	0.56	0.56	0.00	0.00	0.08	0.08	0.00	0.00	0.16	0.16
VPD (Pa)	550.59	684.41	1043.45	492.86	234.36	1436.28	2538.47	2304.11	561.01	1646.96	2450.87	1889.87	75.81	1497.14	2450.87	2375.07
solar rad. (J/day)	1907.66	2479.81	6769.57	4861.91	1907.66	3155.75	6983.82	5076.15	2779.32	3565.14	6399.25	3619.93	2088.41	3565.14	6399.25	4310.84
salinity (PSS)					30.84	33.65	34.07	3.22	33.21	33.65	34.07	0.85	32.94	33.56	34.07	1.13
SST (°C)	9.64	11.93	15.53	5.89	8.71	12.26	17.55	8.84	10.88	13.26	17.55	6.68	10.82	15.33	20.63	9.81
Chlor-*a* (mg m^{-3})	1.81	3.51	9.82	8.01	0.61	2.46	9.82	9.21	0.70	2.39	8.29	7.58	0.24	1.40	8.29	8.05
December																
Air temp. (°C)	6.93	10.41	12.08	5.14	5.38	13.56	19.86	14.48	12.02	15.04	19.86	7.84	11.30	15.77	21.50	10.21
Precipitation (cm/day)	0.31	1.16	2.71	2.4	0	0.41	2.71	2.71	0.00	0.20	1.04	1.04	0.00	0.17	1.63	1.63
VPD (Pa)	296.52	388.65	503.81	207.29	285.51	603.77	1998.98	1713.47	546.61	900.05	1998.98	1452.37	309.71	989.60	2209.94	1900.22
solar rad. (J/day)	1067.43	1327.01	1605.4	537.96	1067.43	1948.7	2679.80	1612.37	1703.24	2287.24	2679.80	976.56	1648.61	2299.03	2812.19	1163.58
salinity (PSS)					28.65	33.26	33.80	5.15	33.02	33.49	33.69	0.66	28.65	33.28	33.80	5.15
SST (°C)	9	10.63	13.0875	4.09	9	12.86	17.16	8.16	10.35	13.52	17.16	6.81	10.28	14.60	19.53	9.26
Chlor-*a* (mg m-3)	1.9	2.82	4.414045	2.51	0.46	1.31	4.80	4.34	0.59	1.18	4.02	3.43	0.25	0.98	4.02	3.77